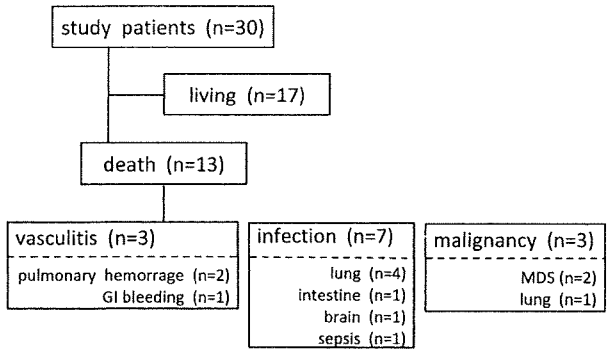

Fig. 2 Causes and number of deaths due to three causes

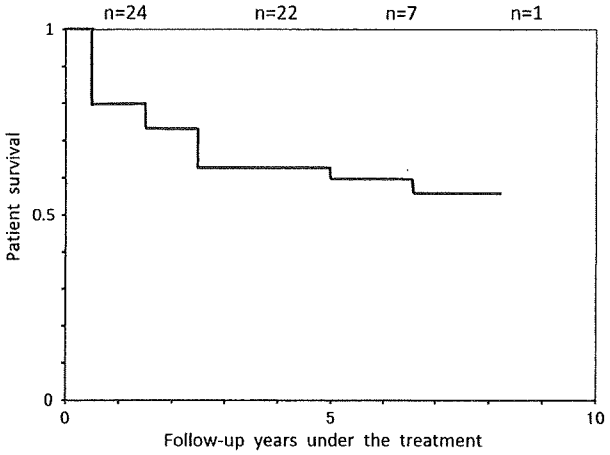

Fig. 3 Table analysis of patient survival. The numbers (for example, $n = 24$) by each *point* indicate the numbers available for analysis by that time

administered to the patients. Death due to infection was observed in seven patients, consisting of four patients with pulmo-renal type, two with pulmonary type, and one with renal type. The focus of these infections was the lungs in four patients, the gut in one, the brain in one, and sepsis in one. The pathogenetic microbes were cytomegalovirus in two patients, *Aspergillus* in two, *Pneumocystis jirovecii* in one, methicillin-resistant *Staphylococcus aureus* in one, *Pseudomonas aeruginosa* in one, and *Mycobacterium avium* in one. Of these infections, one patient had a complicated infection of both *Aspergillus* and cytomegalovirus. These infections occurred from 1 month to 5 years after the postdiagnosis treatment of vasculitis. The infections in three patients were demonstrated within 3 months, whereas in the remaining four patients the infections were detected after 6 months. All of these seven patients died 2–6 months after the occurrence of infections. Death due to malignancy was observed in three patients (two with myelodyscrasia syndrome and one with lung carcinoma), two of whom had pulmo-renal type and one pulmonary type. Two of these patients had received long-term administration of immunosuppressant drugs prior to diagnosis of malignancy, while the remaining patient did not receive any of these drugs.

Kidney prognosis

Ten patients developed chronic renal failure and required hemodialysis. The clinical subtypes of these patients when they underwent hemodialysis were pulmo-renal type in three patients, pulmonary type initially subsequently progressing to pulmo-renal type in five, renal type in one, and systemic type in one. The incubation period to hemodialysis after the diagnosis of vasculitis was within 3 months in nine patients, and 3 years in one patient. The interval from the initial organ involvement to hemodialysis was within 3 months in three patients, 1.5 years in one patient, and more than 3 years in six patients. Another 11 patients had kidney involvement but did not demonstrate end-stage renal disease at the end of the study.

Relapse

Ten patients relapsed, including six patients with pulmo-renal type, three patients with pulmonary type, and one patient with renal type. Time to relapse ranged from 1 to 5 years after diagnosis of vasculitis, and the average time was 2.7 years. All of these patients presented similar symptoms to the original clinical subtypes at time of relapse, except for one patient who showed additional symptoms of CNS involvement (meningitis).

Discussion

Thirty patients, who were hospitalized from 1 January 2001 to 31 December 2004 were observed to evaluate their initial organ involvement, development of clinical features, clinical manifestations on admission, patient survival, kidney prognosis, and relapse. The classification of ten clinical subtypes in addition to pulmo-renal type was applied to the study patients for the analysis of the above-mentioned events. The results disclosed that, when the initial organ involvement excluding constitutional manifestations were evaluated, pulmonary manifestations were found in 20 patients (66.7%), the most common symptom. Renal involvement was observed in 13 patients (43.3%) and was the second most common. The other initial organ involvements included peripheral neuritis in three patients (10.0%), muscle-articular ache in one patient (3.3%), ENTE features in one patient (3.3%), and systemic

well as peripheral neuropathy in addition to lung and kidney involvement [2, 3]. When the patients are seen at the time that MPO-ANCA-associated vasculitis is diagnosed, they do not necessarily present with the full-blown manifestations in all organs. The relationship between the clinical manifestations and patient survival in this disease has been described in some previous reports; for example, the important prognostic factors for patient survival have been described to be pulmonary hemorrhage, gastrointestinal bleeding or perforation, brain hemorrhage or thrombosis, and myocardial infarction [2, 4, 5]. Kidney prognosis has also been reported to be associated with percentage of crescent formation, increased number of sclerotic glomeruli, widening of tubulointerstitial fibrosis, and patient age [6–8]. However, these reports did not pay much attention to the relationship of early manifestation of the disease with the eventual clinical development as well as patient survival. Under these circumstances, hospitalized patients at our university hospital, who were thoroughly evaluated historically, physically, and based on laboratory investigations on admission, were categorized into ten clinical subtypes and then followed up over more than 2 years for eventual patient survival, kidney prognosis, and relapse. After making a diagnosis, the patients were treated with the recommended treatment as suggested by the Research Committee for Refractory Vasculitis Syndrome [9]. The results of the study disclosed some interesting new relationships between the classification of clinical subtypes and patient survival, kidney prognosis, as well as relapse in Japanese patients with MPO-ANCA-associated vasculitis.

Materials and methods

Study patients

Thirty patients, who were hospitalized in the First Department of Internal Medicine, Kyorin University, from 1 January 2000 to 31 December 2004 and were subsequently followed up for more than 2 years, were enrolled in this study. Any patients that died during the course of the study were excluded at that time, but their data prior to death were used for the clinical analysis. This study was ended on 31 December 2006. Patient ages ranged from 54 to 91 years old and their mean age was 69.2 years. The male-to-female ratio was 9:21. In addition to obtaining the precise history of their illness, urinalysis and serum creatinine level data were confirmed using health check sheets. Furthermore, if the patients had been previously treated by their family physicians, then all records of physical examination, chest X-ray, and blood chemistry were obtained for this study.

Diagnosis and the time interval for diagnosis

Diagnosis

Because of the difficulty in obtaining biopsy tissue specimens for the diagnosis of vasculitis from every patient, the diagnosis for MPO-ANCA-associated vasculitis was dependent on the positivity of MPO-ANCA as well as the existence of organ involvement due to vasculitis. The MPO-ANCA test was performed by the enzyme-linked immunoassay reagent produced by Nipro Company (Shiga, Japan) [10]. The common vasculitis symptoms and findings in each organ are listed in the Appendix. However, small-vessel vasculitic diseases of the connective tissues disorder such as systemic lupus erythematosus, Henoch-Schönlein purpara, Churg-Strauss syndrome, cryoglobulinemia, Wegener's granulomatosis, Sjögren syndrome, and Goodpasture syndrome were excluded from this study based on all of the diagnostic criteria as well as no apparent positivity of MPO-ANCA in these diseases.

The time interval for diagnosis

This was defined as the number of months or years between the onset of the initial organ symptoms and the diagnosis of MPO-ANCA-associated vasculitis. Because it was difficult to obtain a clear-cut history of the illness for most of the patients, the time interval after the first symptoms was estimated to be as follows: 0 months when the diagnosis was made less than 3 months later, 0.5 years when the diagnosis was made 4–9 months later, 1 year when the diagnosis was made 9–12 months later, and the required years when the diagnosis was made more than 1 year later.

Initial organ involvement and the definition of the observation period

Initial organ involvement was determined as the major clinical symptom and/or laboratory data which necessitated the patient to be seen by their physicians on at least three consecutive occasions. However, constitutional symptoms such as fever, fatigue or weight loss were excluded in the determination of initial organ involvement, because there were no organ-related symptoms. The definition of the observation period was the length of time that the patient was observed without receiving any appropriate treatment for vasculitis, calculated on a year(s) basis.

Clinical subtypes and their development during the observation period, and the clinical subtypes on admission

The clinical subtype of the patients was classified into pulmonary, renal, gastrointestinal, cardiovascular, CNS,

Appendix

Common vasculitis symptoms and findings in each organ.

1. Pulmonary: hemoptysis, pulmonary hemorrhage, interstitial pneumonitis, interstitial fibrosis
2. Renal: rapidly progressive glomerulonephritis, glomerulonephritis (proteinuria and/or RBCs in the sediment)
3. Gastrointestinal: abdominal pain with bloody stool or moderate—strong occult blood in the stool, epigastric pain or right upper quadrant pain associated with increased serum amylase and/or elevated liver enzymes
4. Cardiovascular: angina pectoris, myocarditis, myocardial infarction, pericarditis, aortitis
5. CNS: infarction, hemorrhage, meningitis
6. Peripheral neuritis: mononeuritis multiplex
7. Musculo-articular: muscle pain/tenderness, arthralgia, arthritis
8. ENTE: E, otitis media refractory to antibiotics, sudden onset of inner ear deafness; N, refractory rhinitis with epistaxis and/or nonpathognomonic bacterial growth purulent discharge; T, ulcer in the ororhinopharyx or larynx; E, episcleritis, iritis, uveitis, retinitis
9. Dermatologic: palpable purpura, ecchymosis, skin ulcer
10. Systemic type: involving more than three vital organs. Vital organs include lung, kidney, gastrointestinal tract, gallbladder, pancreas, liver, heart, CNS.

References

1. Jennette JC, Falk RJ, Andrassy K, Bacon P, Churg J, Gross WL, et al. Nomenclature of systemic vasculitis. Proposal of an international consensus conference. Arthritis Rheum. 1994;37:187–92.
2. Falk RJ, Hogan S, Carey TS, Jennette JC, the Glomerular Disease Collaborative Network. Clinical course of antineutrophil cytoplasmic autoantibody-associated glomerulonephritis and systemic vasculitis. Ann Intern Med. 1990;113:656–63.
3. Geffriand-Ricouard C, Noel LH, Chauveau D, Houhou S, Grundfeld JP, Lesavre P. Clinical spectrum associated with ANCA defined antigen specificities in 98 selected patients. Clin Nephrol. 1993;39:125–36.
4. Hogan S, Nachman PH, Wilkman AS, Jennette JC, Falk RJ, the Glomerular Disease Collaborative Network. Prognostic markers in patients with antineutrophil cytoplasmic autoantibody-associated microscopic polyangiitis and glomerulonephritis. J Am Soc Nephrol. 1996;7:23–32.
5. Westman KWA, Bygren PG, Olsson H, Ranstam J, Wieslander J. Relapse rate, renal survival, and cancer morbidity in patients with Wegener's granulomatosis or microscopic polyangiitis with renal involvement. J Am Soc Nephrol. 1998;9:842–52.
6. Bajema IM, Hogan EC, Hermans J, Noël LH, Waldherr R, Ferrario F, et al. Kidney biopsy as a predictor for renal outcome in ANCA-associated necrotizing glomerulonephritis. Kidney Int. 1999;56:1751–8.
7. Kawamoto S, Kawamura T, Utsunomiya Y, Kawaguchi Y, Hosoya T. Analysis of risk factor for patients and renal survival in anti-myeloperoxidase antibody (MPO-ANCA) associated glomerulonephritis (in Japanese, abstract in English). Jpn J Nephrol. 1999;41:719–25.
8. Hauer HA, Bajema IM, van Houwelingen HC, Ferrario F, Noël LH, Waldherr R, et al. Determinants of outcome in ANCA-associated glomerulonephritis: a prospective clinico-histopathological analysis of 96 patients. Kidney Int. 2002;62:1732–42.
9. Japanese Study Group for MPO-ANCA-Associated Vasculitis (JMAAV). The prospective cohort study for MPO-ANCA associated vasculitis treated according to the standard protocol regimen (directed by Prof S.Ozaki, in Japanese). 2006 Annual Report on Intractable Vasculitis Syndrome supported by the Ministry of Health, Welfare, and Labour of Japan; 2006. pp. 199–273.
10. Nagakawa T, Arimura Y, Yoshida M, Hiromura N, Naruse T, Nishiki N, et al. Fundamental and clinical evaluation of MPO ELISA kit (NISSHO) (in Japanese). Lab Mach Reag. 1995; 18:127–35.
11. Gordon M, Luqmani RA, Adu D, Greaves I, Richards N, Michael J, et al. Relapses in patients with a systemic vasculitis. Q J Med. 1993;86:779–89.
12. Nachman PH, Hogan SL, Jennette JC, Falk RJ. Treatment response and relapse in antineutrophil cytoplasmic auto-antibody associated microscopic polyangiitis and glomerulonephritis. J Am Soc Nephrol. 1996;7:33–4.
13. Nakabayashi K, Kobayashi S, Matsuoka Y, Yoshida T, Yoshida M, Ozaki S, et al. Statistical analysis of infectious death in patients receiving immunosuppressive drugs with medium-and small-vessel vasculitides (in Japanese, abstract in English). 2000 Annual Report for the Refractory Vasculitis Syndrome (Chief: prof H. Hashimoto) supported by Ministry of Health, Welfare, and Labour of Japan; 2001. pp. 58–68.
14. Sakai H, Kurokawa K, Koyama T, Arimura Y, Kida H, Shigematsu S, et al. The treatment guideline for rapidly progressive glomerulonephritis (in Japanese). Jpn J Nephrol. 2002;44:55–82.
15. Fujii A, Tomizawa K, Arimura Y, Nagasawa T, Uhashi YY, Hiyama S, et al. Epitope analysis of myeloperoxidase (MPO) specific anti-neutrophil cytoplasmic autoantibodies (ANCA) in MPO-ANCA-associated glomerulonephritis. Clin Nephrol. 2000; 53:242–52.

Am J Physiol Renal Physiol 298: F133–F141, 2010.
First published November 11, 2009; doi:10.1152/ajprenal.00400.2009.

Histone deacetylase modulates the proinflammatory and -fibrotic changes in tubulointerstitial injury

Takeshi Marumo,[1,2] Keiichi Hishikawa,[1,2] Masahiro Yoshikawa,[1,2] Junichi Hirahashi,[2] Shoji Kawachi,[3] and Toshiro Fujita[1,2]

[1]*Department of Clinical Renal Regeneration,* [2]*Division of Nephrology and Endocrinology, Department of Internal Medicine, University of Tokyo, and* [3]*Surgical Operation Department, International Medical Center of Japan, Tokyo, Japan*

Submitted 15 July 2009; accepted in final form 4 November 2009

Marumo T, Hishikawa K, Yoshikawa M, Hirahashi J, Kawachi S, Fujita T. Histone deacetylase modulates the proinflammatory and -fibrotic changes in tubulointerstitial injury. *Am J Physiol Renal Physiol* 298: F133–F141, 2010. First published November 11, 2009; doi:10.1152/ajprenal.00400.2009.—Histone deacetylase (HDAC) regulates gene expression by modifying chromatin structure. Although changes in the expression and activities of HDAC may affect the course of kidney disease, the role of HDAC in tubulointerstitial injury has not been explored. We therefore investigated the alterations in HDAC expression and determined the effects of HDAC inhibition on the tubulointerstitial injury induced by unilateral ureteral obstruction. The induction of HDAC1 and HDAC2, accompanied by a decrease in histone acetylation was observed in kidneys injured by ureteral obstruction. Immunohistochemical analysis revealed that HDAC1 and HDAC2 were induced in renal tubular cells. Treatment with an HDAC inhibitor, trichostatin A (TSA), attenuated macrophage infiltration and fibrotic changes in tubulointerstitial injury induced by ureteral obstruction. The induction of colony-stimulating factor-1 (CSF-1), a chemokine known to be involved in macrophage infiltration in tubulointerstitial injury, was reduced in injured kidneys from mice treated with TSA. TSA, valproate, and the knockdown of HDAC1 or HDAC2 significantly reduced CSF-1 induced by TNF-α in renal tubular cells. These results suggest that tubular HDAC1 and HDAC2, induced in response to injury, may contribute to the induction of CSF-1 and the initiation of macrophage infiltration and profibrotic responses. These findings suggest a potential of HDAC inhibition therapy aimed at reducing inflammation and fibrosis in tubulointerstitial injury.

epigenetic; chemokine; ureteral obstruction

EPIGENETIC MECHANISMS INCLUDING changes in histone acetylation have recently been suggested to be involved in altered gene expression in various pathological conditions, including cancer (33), cardiac hypertrophy (4), chronic obstructory pulmonary disease (14), denervation (24), and recovery of learning and memory after neuronal loss (10). Changes in histone acetylation, which are controlled by histone deacetylase (HDAC) and histone acetyltransferase, regulate gene transcription by altering chromatin structure. The distinct roles of each HDAC isozyme in such pathological conditions have recently begun to be revealed (11, 12, 28, 29, 36). Despite the potential role of HDAC in molecular responses to kidney injury, changes in the expression of HDAC and histone acetylation in the kidney have not been characterized. In this regard, we recently reported that HDAC5 downregulation, which leads to histone acetylation in renal tubular cells, contributes to the regenerative response to ischemia (21).

The importance of changes in HDAC activity and histone acetylation in kidney disease has also been indicated by the observations by us and others that the HDAC inhibitor reduced glomerular lesions and proteinuria in models of lupus nephritis (26) and anti-glomerular basement membrane glomerulonephritis (13). In addition to glomerulonephritis, our previous in vitro observation suggested that tubulointerstitial injury can also be a direct target of HDAC inhibitors independently of glomerular lesions, since an HDAC inhibitor, trichostatin A (TSA), attenuates the epithelial-to-mesenchymal transition induced by transforming growth factor (TGF)-β in cultured renal tubular cells (42).

The infiltration of inflammatory cells into the interstitial space in the kidney is one of the earliest events in tubulointerstitial injury and regulates fibrosis and tubular atrophy (1, 8). In response to injury, renal tubular cells express several chemokines that induce the migration of inflammatory cells into the interstitium. Although the contribution of a subset of macrophages in the resolution of renal injury needs to be clarified in each pathological condition (31), the inhibition of initial macrophage influx by the blockade of some of the intrarenal chemokines, such as monocyte chemoattractant protein (MCP)-1 (2, 19) and colony-stimulating factor (CSF)-1 (16, 20), has been shown to attenuate tubulointerstitial injury induced by ureteral obstruction.

In the present study, we investigated the changes in HDAC expression and histone acetylation in kidney injured by unilateral ureteral obstruction (UUO), a model of tubulointerstitial injury characterized by inflammation and fibrosis that is independent of glomerular lesions. We further determined the effects of HDAC inhibition on the early stages of inflammatory and fibrotic changes induced by UUO.

MATERIALS AND METHODS

UUO injury. Seven- to eight-week-old male C57BL/6J mice (Tokyo Laboratory Animal Center, Tokyo, Japan) were fed a standard laboratory diet (MF; Oriental Yeast, Tokyo, Japan) and water ad libitum. The left ureter was exposed through the flank and completely ligated with 4.0 silk under anesthesia with pentobarbital sodium (50 mg/kg ip). Mice were randomly assigned to two groups and were treated as follows. The TSA-treated group was composed of animals treated with 10 mg/kg of TSA, which was administered by intraperitoneal injection daily for 2 or 5 days. The vehicle-treated group was composed of animals treated with dimethylsulfoxide instead of TSA. Two or five days after UUO, the kidneys were perfused with saline and removed from animals under anesthesia with pentobarbital sodium. For the morphological analysis and immunohistochemical analysis of α-smooth muscle actin (SMA), a marker of myofibroblasts,

Address for reprint requests and other correspondence: T. Marumo, Dept. of Clinical Renal Regeneration, and Div. of Nephrology and Endocrinology, Dept. of Internal Medicine, Univ. of Tokyo, 7-3-1 Hongo, Bunkyo-ku, 113-8655 Tokyo, Japan (e-mail: tmarumo-npr@umin.ac.jp).

表 1 Incidence and demographics of primary systemic vasculitides

Location, Country [reference number]	Latitude	mean age	M vs. F	Annual incidence (/million)				Study period
				MPA	WG	CSS	total	
Tromso, Norway[6]	70°N	ND	ND	2.7	10.5	0.5	13.7	1988～1998
Norwich, United Kingdom[7]	52°N	62.9 yr	1.3 vs. 1	8.0	9.7	2.7	ND	1988～1998
Schleswig-Holstein, Germany[8]	51°N	60.5 yr	1.0 vs. 1	2.7	7.9	1.1	11.7	1998～2002
Lugo, Spain[9]	43°N	60.7 yr	1.2 vs. 1	7.9	3.0	1.3	12.2	1988～2001

MPA：microscopic polyangiitis, WG：Wegener's granulomatosis, CSS：Churg-Strauss syndrome

表 2 Inclusion criteria

1. New patients with WG, MPA, CSS, or RLV, with or without histological confirmation*
2. Renal involvement**with or without other organ involvements, attributable to active WG, MPA, CSS, or RLV
3. Positive serology for ANCA***

1, 2 and 3 are required.

*Histological confirmation：findings of necrotizing vasculitis and pauci-immune necrotizing, crescentic glomerulonephritis

**Renal involvement：elevated serum creatinine (>1.3 mg/dL), or hematuria (>30 red blood cells per high power field), or proteinuria (>1 g/24h), or red cell casts

***ANCA negativity is allowed if the disease is confirmed histologically.

WG：Wegener's granulomatosis, MPA：microscopic polyangiitis, CSS：Churg-Strauss syndrome, RLV：renal limitted vasculitis

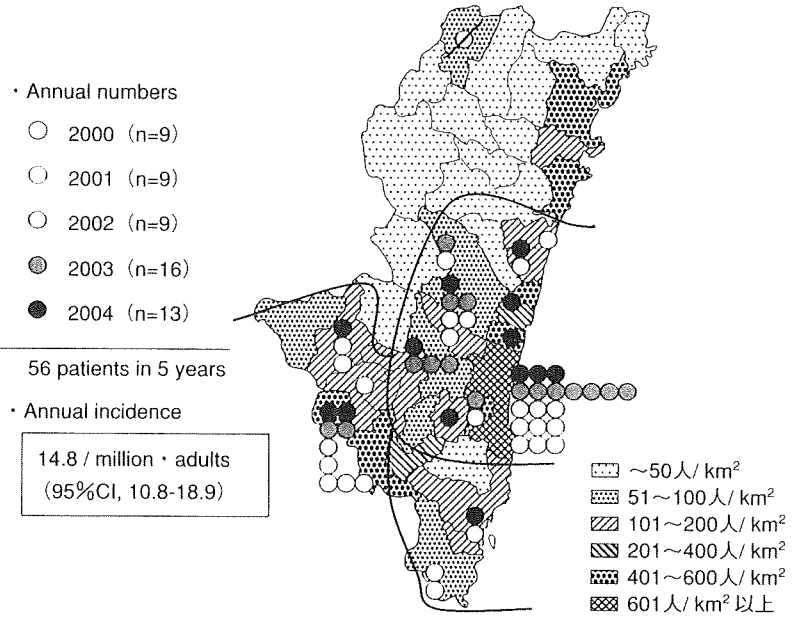

図 Distribution of the patients with ANCA-associated renal vasculitis between 2000 and 2004 in the Miyazaki prefecture

いが，発症率に関するものは少ない。

一方，本邦からは，rheumatologists を中心とした厚生労働省血管炎研究班からの血管炎全国アンケート調査の集計に基づく罹患率の報告がある[10]。それによると，年間 100 万人当たりの罹患者数は，MPA 13.8 例，WG 2.3 例，CSS 1.0 例であり，これらの 3 疾患全体では 17.1 例と報告されている。このなかには腎症を伴わない患者も含まれている。さらに nephrologists を主体とした厚生労働省進行性腎障害研究班からの RPGN 全国アンケート調査が行われており，本邦の RPGN の詳細が明らかにされている[11,12]。

このように，調査方法，対象疾患，調査の施行者などが異なることから，一概には疾患頻度を比較することは困難である。

本邦の ANCA 関連腎血管炎の発症率

われわれは，ヒューマンサイエンス財団から研究助成を受けて発足された「抗好中球細胞質抗体(ANCA)関連血管炎の本邦・欧州間での臨床疫学調査および診断薬と治療法開発に関する研究」の研究班(主任研究者：橋本博史，2004～2006 年)において，宮崎県における ANCA 関連腎血管炎の発症率の調査を行った(a retrospective, population-based study)。ANCA 関連腎血管炎の症例抽出にあたっては，EUVAS グループに倣って表 2 の条件を満たす例とした。2000 年 1 月～2004 年 12 月の 5 年間に 56 例の症例が検出され(図)，成人(≧15 歳)では 1 年間に人口 100 万人当たり 14.8 例(95 %CI 10.8-18.9)，高齢者(≧65 歳)では 44.8

vasculitis in one patient (3.3%). These data suggest that lung and kidney symptoms are the most common manifestation in this disease, even in the early phase of the disease, as partly described in the literature [1–3]. The time interval from the first organ symptoms to the diagnosis was within 3 months in 12 patients (40%), within 1 year in 9 patients (30%), and more than 2 years in 9 patients (30%). Accordingly, two-thirds of the patients were diagnosed within 1 year of the initial organ symptoms, whereas the patients with pulmonary fibrosis, but who were not associated with any other organ symptoms, were not diagnosed more than 2 years after the initial pulmonary manifestation. Therefore, when any type of pulmonary fibrosis is found, MPO-ANCA should be considered for the etiologic diagnosis.

Development of clinical subtypes during the observation period was also studied over an average period of 4.3 years. Twenty-one patients (70%) remained in the same clinical subtypes, whereas nine patients (30%) added new clinical symptoms during the observation period. The five patients with development showed pulmonary type initially and eventually progressed to pulmo-renal type. The remaining two patients, who manifested pulmonary type initially, subsequently progressed to systemic type, adding kidney and gastrointestinal symptoms. The other two patients, who had renal or ENTE type at first, eventually transformed to pulmo-renal type or ENTE plus pulmo-renal type, respectively. These developments of clinical features during the observation period mean that pulmonary type frequently progresses to pulmo-renal or systemic type, but the other types rarely go into the other types over approximately 4 years of observation. No reports have mentioned this kind of phenomenon in the literature to data, although a few articles discuss in which type of pulmonary involvement has poor prognosis for patient survival [2, 4, 12]. The clinical manifestations on admission were almost the same as the developmental findings of clinical features during the observation period, because all patients were hospitalized around the time of clinical development.

Patient death in this study was found to be related to vasculitis, infections or malignancy. Vasculitic death occurred in patients with systemic type and within 6 months and was due to pulmonary hemorrhage in two patients and gastrointestinal bleeding in one patient. Death due to infection was observed in seven patients; the pathogenetic organisms were opportunistic in nature. These infectious deaths were observed in four patients with pulmo-renal type and two patients with pulmonary type. These infections occurred within 3 months of vasculitis treatment or between 6 months and 5 years after the treatment. Death due to malignancy was observed in two patients with myelodyscrasia syndrome and one with pulmonary carcinoma. These deaths were in two patients with pulmo-renal type and one patient with pulmonary type. These data imply that early postdiagnosis death is associated with vasculitis itself, that infectious death occurring at various times is opportunistic and is associated with the steroid treatment as well as the old age of the patients, and that death due to malignancy is related to aging but not to treatment. These observations are closely consistent with previous reported findings [2, 4, 5, 12, 13]. However, these data were mostly reported from Europe or the USA, except for one article from our country [13].

Regarding kidney prognosis, one-third of the patients (ten patients) went onto hemodialysis and nine of them were of pulmo-renal type at the time of hemodialysis. The start of hemodialysis in nine patients was within 3 months after the diagnosis. However, after initial organ involvement, three patients needed hemodialysis within 3 months, while six patients required it after more than 3 years. These six patients, who did not require hemodialysis for more than 3 years, showed pulmonary fibrosis as the initial organ involvement and eventually developed to pulmo-renal type, resulting in end-stage renal failure. These features suggest that the pulmo-renal type has a high incidence of progression to renal failure, as is partly supported by the findings of a previous analytical article which was published in the *Journal of Clinical and Experimental Nephrology* by the Study Group for Rapidly Progressive Glomerulonephritis in Japan [14].

A relapse was observed in ten patients, who mainly had pulmo-renal or pulmonary type. Relapse occurred about 2.7 years after the diagnosis of vasculitis and most of the relapses were manifested with similar symptoms to the original clinical subtypes. The relapse time and rate were almost the same as in data described in previous articles [5, 11]. This similarity between relapse features and previous manifestations was also documented in other studies [2, 12]. These recurrent appearances of similar features in relapse are in accordance with the study of MPO epitopes analysis in MPO-ANCA vasculitis, which suggests the existence of different MPO epitopes in the different clinical subtypes [15].

Based on these analytical data, we can conclude that this classification of clinical subtypes at the initial time and on admission is meaningful to some extent for predicting patient survival, kidney prognosis, and relapse in the future as well as to help to identify the appropriate treatment.

Acknowledgments This article is supported in part by grants (2000–2007) of the Research Committee of Refractory Vasculitis Syndrome sponsored by the Ministry of Health, Welfare, and Labor of Japan.

一されて，国際的な視野でさらにこの疾患の特徴が明らかにされ治験が進んでいくことが期待される。

文　献

1. Jayne DRW, Rasmussen N. Treatment of anti-neutrophil cytoplasmic antibody-associated systemic vasculitis：Initiatives of the European Community Systemic Vasculitis Clinical Trial Study Group. Mayo Clin Proc 1997；72：737-747.
2. Jayne DRW；European Vasculitis Study Group (EUVAS). Update on the European Vasculitis Study Group trials. Curr Opin Rheumatol 2001；13：48-55.
3. Hunder GG, Arend WP, Bloch DA, et al. The American College of Rheumatology 1990 criteria for classification of vasculitis. Arthritis Rheum 1990；33：1065-1072.
4. Jennette JC, Falk RJ, Andrassy K, et al. Nomenclature of systemic vasculitides. Proposal of an international consensus conference. Arthritis Rheum 1994；37：187-192.
5. 厚生科学研究特定疾患対策研究事業　難治性血管炎に関する調査研究班(班長：橋本博史)．難治性血管炎の診療マニュアル．2002年3月．
6. Watts RA, Lane SE, Scott DG, Koldings W, Nossent H, Gonzalez-Gay MA, Garcia-Porrua C, Bentham GA. Epidemiology of vasculitis in Europe. Ann Rheum Dis 2001；60：1156-1157.
7. Watts RA, Lane SE, Bentham G, Scott DG. Epidemiology of systemic vasculitis：a ten-year study in the United Kingdom. Arthritis Rheum 2000；43：414-419.
8. Reinhold-Keller E, Herlyn K, Wagner-Bastmeyer R, Gross WL. Stable incidence of primary systemic vasculitides over five years：Results from German vasculitis register. Arthritis Rheum 2005；53：93-99.
9. Gonzalez-Gay MA, Garcia-Porrua C, Guerrero J, Rodriguez-Ledo P, Llorca J. The epidemiology of the systemic vasculitides in northwest Spain：Implications of the Chapel Hill Consensus Conference Definitions. Arthritis Rheum 2003；49：388-393.
10. 松本美富士，小林茂人，橋本博史，他．日本における難治性血管炎の全国疫学調査．In：厚生省特定疾患に関する疫学調査研究班，1998年度研究報告書．1998：15-23.
11. 堺　秀人，黒川　清，小山哲夫，他(急速進行性糸球体腎炎診療指針作成合同委員会)．急速進行性腎炎症候群の治療指針．日腎会誌 2002；44：55-83.
12. 山縣邦弘，小山哲夫．ANCA関連腎炎の概念と定義　疫学．長澤俊彦(編)新しい診断と治療のABC．31 ANCA関連腎炎(最新医学別冊)．東京：最新医学社，2005：15-23.
13. Fujimoto S, Uezono S, Hisanaga S, Fukudome K, Kobayashi S, Suzuki K, Hashimoto H, Nakao H, Nunoi H. Incidence of ANCA-associated primary renal vasculitis in the Miyazaki prefecture：The first population-based, retrospective, epidemiologic study in Japan. Clin J Am Soc Nephrol 2006；1：1016-1022.
14. Satchell SC, Nicholls AJ, D'Souza RJ, Beaman M. Renal vasculitis：increasing a disease of the elderly? Nephron Clin Prac 2004；97：c142-c146.
15. Lane SE, Scott DG, Heaton A, Watts RA. Primary renal vasculitis in Norfolk—increasing incidence or increasing recognition? Nephrol Dial Transplant 2000；15：23-27.
16. Tidman M, Olander R, Svalander C, Danielsson D. Patients hospitalized because of small vessel vasculitides with renal involvement in the period 1975-1995：organ involvement, ANCA patterns, seasonal attack rates and fluctuation of annual frequencies. J Intern Med 1998；244：133-141.
17. Watts RA, Scott DGI, Jayne DRW, Ito-Ihara T, Muso E, Fujimoto S, Harabuchi Y, Kobayashi S, Suzuki K, Hashimoto H. Renal vasculitis in Japan and the UK—are there differences in epidemiology and clinical phenotype? Nephrol Dial Transplant 2008；23：3928-3931.
18. Hogan SL, Nachman PH, Wilkman AS, Jennette JC, Falk RJ；Glomerular Disease Collaborative Network. Prognostic markers in patients with antineutrophil cytoplasmic autoantibody-associated microscopic polyangiits and glomerulonephritis. J Am Soc Nephrol 1996；7：23-32.
19. Hauer HA, Bajema IM, Van Houwelingen HC, Ferrario F, Noel LH, Waldherr R, Jayne DRW, Rasmussen N, Bruijn JA, Hagen C. Renal histology in ANCA-associated vasculitis：Differences between diagnostic and serologic subgroups. Kidney Int 2002；61：80-89.
20. Booth AD, Almond MK, Burns A, Ellis P, Gaskin G, Neild GH, Plaisance M, Pusey CD, Jayne DRW. Outcome of ANCA-associated renal vasculitis：A 5-year retrospective study. Am J Kidney Dis 2003；41：776-784.
21. Tsuchiya N, Kobayashi S, Kawasaki A, Kyogoku C, Arimura Y, Yoshida M, Tokunaga K, Hashimoto H. Genetic background of Japanese patients with antineutrophil cytoplasmic antibody-associated vasculitis：association of HLAA-DRB1*0901 with microscopic polyangiitis. J Rheumatol 2003；30：1534-1540.
22. Fujii A, Tomizawa K, Arimura Y, Nagasawa T, Ohashi YY, Hiyama T, Mizuno S, Suzuki K. Epitope analysis of myeloperoxidase-(MPO) specific anti-neutrophil cytoplasmic autoantibodies (ANCA) in MPO-ANCA-associated glomerulonephritis. Clin Nephrol 2000；53：242-252.
23. Lane SE, Watts RA, Bentham G, Innes NJ, Scott DG. Are environmental factors important in primary systemic vasculitis? A case-control study. Arthritis Rheum 2003；48：814-823.
24. Beaudreuil S, Lasfargues G, Laueriere L, Ghoul ZE, Fourquet F, Longuet C, Halimi JM, Nivet H, Buchler M. Occupational exposure in ANCA-positive patients：a case-control study. Kidney Int 2005；67：1961-1966.
25. Ito-Ihara T, Muso E, Kobayashi S, Uno K, Tamura N, Yamanishi Y, Fukatsu A, Watts RA, Scott DGI, Jayne DRW, Suzuki K, Hashimoto H. A comparative study of the diagnostic accuracy of ELISA for the detection of anti-neutrophil cytoplasma antibodies available in Japan and Europe. Cli Exp Rheum 2008；26：1027-1033.

levels of 18S rRNA and expressed as relative values to those obtained with control.

Renal tubular cell culture and RNA interference for knockdown of HDAC1 and HDAC2. The normal rat kidney epithelium-derived cell line NRK 52E was obtained from the American Type Culture Collection and grown in DMEM with 5% FBS in a humidified 5% CO_2-95% air environment at 37°C. Subconfluent NRK 52E cells were transfected with 33 nM HDAC1 or HDAC2 Stealth RNAi (RNA interference; Invitrogen Japan, Tokyo, Japan), or Stealth RNAi Negative Control Duplex (Lo GC Duplex, Invitorgen) using Lipofectamine RNAiMAX (Invitrogen) in accordance with the manufacturer's instructions. The sequences employed were as follows: HDAC1 sense, 5′-CGGCAUUGAUGAUGAGUCCUAUGAA-3′, antisense, 5′-UUCAUAGGACUCAUCAUCAAUGCCG-3′; and HDAC2 sense, 5′-CCUAACUGUCAAAGGUCACGCUAAA-3′, antisense, 5′-UUUAGCGUGACCUUUGACAGUUAGG-3′. After 24 h of incubation with the RNAi, cells were then treated with or without TNF-α for 24 h.

Statistics. All data are expressed as means ± SE. Multiple parametric comparisons were performed by analysis of variance, followed by Fisher's protected least significant difference test. Comparisons between two groups were performed by Student's *t*-test. Values of $P < 0.05$ were considered statistically significant.

RESULTS

Decrease in histone acetylation accompanied by an increase in HDAC1 and HDAC2 in injured kidneys. UUO-induced kidney injury produced a marked decrease in the level of histone acetylation compared with that in the contralateral kidneys (Fig. 1*A*). Since HDACs are major determinants of histone acetylation levels, we analyzed the changes in the mRNA levels of HDACs in the injured kidneys. The mRNA levels of HDAC1, HDAC2, and HDAC7 were increased in the injured kidneys, whereas those of HDAC3, HDAC4, HDAC5, and HDAC6 remained unchanged compared with those in the contralateral kidneys (Fig. 1*B*). In parallel with the changes in the mRNA levels, the protein levels of HDAC1 and HDAC2 increased in the obstructed kidneys (Fig. 1, *C* and *D*). These observations suggest that the upregulation of HDAC1 and HDAC2 may, at least in part, be involved in a decrease in histone acetylation level in the injured kidneys. In contrast to HDAC1 and HDAC2, however, the HDAC7 protein level was paradoxically decreased in the injured kidneys (Fig. 1*E*). The cause of this discrepancy between the HDAC7 mRNA and protein levels is unknown, but we suspect the possible degradation of HDAC7 protein and the subsequent upregulation of mRNA through a feedback mechanism in the injured kidneys. While further investigation of these changes in HDAC7 is of interest, we rather decided to concentrate on the upregulation of HDAC1 and HDAC2 in the present report, as these changes may contribute to histone deacetylation in the injured kidneys. Induction of HDAC1 and HDAC2 mRNA was estimated to occur in the early stage of injury since the mRNA levels reached the peak at 2 days after UUO treatment (Fig. 1*F*).

To determine the intrarenal changes in HDAC1 and HDAC2, we next performed immunohistochemical analysis. The expression of HDAC1 was observed in the nuclei of tubular and glomerular cells in uninjured kidneys, but some tubular cells did not stain positive for HDAC1 (Fig. 2, *A* and *B*, arrowheads). In contrast, strong staining for HDAC1 was observed in the tubular cells of the injured kidneys (Fig. 2, *C* and *D*). HDAC1 negative cells were rarely observed in the tubular cells of the injured kidneys. HDAC2 staining was less pronounced than HDAC1 staining, but significant HDAC2 staining was observed in the nuclei of tubular and glomerular cells in the contralateral kidneys (Fig. 2, *E* and *F*). In the injured kidneys, strong HDAC2 staining was observed in some tubular cells (Fig. 2, *G* and *H*, arrows). Cell counting analysis revealed that the percentage of tubular cells positive for HDAC1 and HDAC2 was significantly increased in the injured kidneys compared with that in the contralateral kidneys (Fig. 2, *I* and *J*). These observations indicate that HDAC1 and HDAC2 are induced in tubular cells in response to UUO.

Histone deacetylase inhibitor ameliorates fibrotic changes. Based on the results that histone deacetylation and the upregulation of HDAC1 and HDAC2 are induced in the early stage of UUO, we next determined the effects of an HDAC inhibitor, TSA, on the early fibrotic changes observed in the injured kidneys. TSA markedly decreased the interstitial fibrosis induced by UUO (Fig. 3, *A–C*). The fibrosis score was significantly reduced in the obstructed kidneys of the mice treated with TSA compared with the samples obtained from animals treated with vehicle (Fig. 3*D*). In accordance with the results obtained using Masson's trichrome staining, the area positive for α-SMA was significantly reduced by TSA treatment (Fig. 3, *E–H*). Western blot analysis revealed that the protein levels of α-SMA in obstructed kidneys were attenuated by ~15% in TSA-treated mice (Fig. 4*A*). In addition, an increase in the mRNA level of collagen 1a and α-SMA induced by UUO was significantly attenuated by TSA (Fig. 4, *B* and *C*). TSA treat-

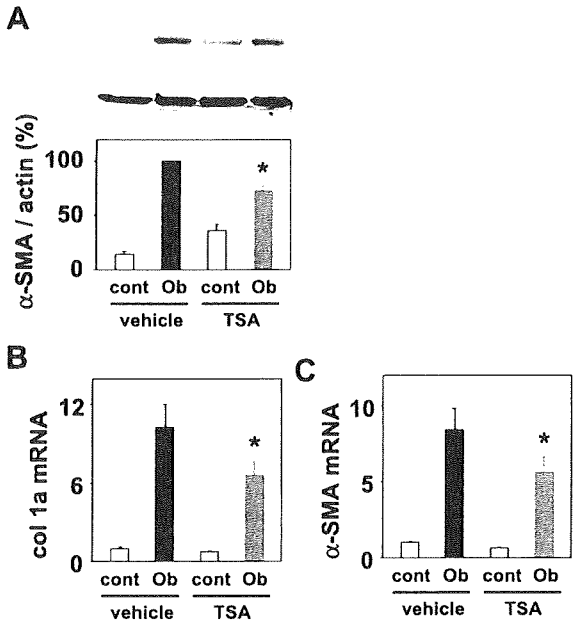

Fig. 4. Reduction in fibrotic markers in UUO mice by HDAC inhibition. The protein levels of α-SMA (*A*) in kidneys obtained 2 days after ureteral obstruction from mice treated with vehicle or TSA were determined by Western blot analysis. Representative films of Western blot analysis for α-SMA are shown at the *top*. Blots for β-actin are shown in the *middle*. The results of densitometric analysis are shown at the *bottom*. Values are means ± SE ($n = 4$). The mRNA levels of collagen 1a (*B*) and α-SMA (*C*) in kidneys obtained 2 days after ureteral obstruction from mice treated with vehicle or TSA were determined by RT-PCR. Values were normalized to those for 18S and expressed as relative values of contralateral kidneys obtained from mice treated with vehicle. Values are means ± SE ($n = 7–8$). *$P < 0.05$ vs. values of obstructed kidneys obtained from mice treated with vehicle.

Table 1. *Primer sequences for RT-PCR*

Primer	Sequence of PCR Primers	GenBank Accession No.
Mouse HDAC1		NM_008228
Forward	5′-CTCAGGGCACCAAGAGGAAAG-3′	
Reverse	5′-TTGAGCAGCAAATTGTGAGTCA-3′	
Mouse HDAC2		NM_008229
Forward	5′-TGCTTGCCATCCTCGAATTACT-3′	
Reverse	5′-GTCATCACGCGATCTGTTGTATAAA-3′	
Mouse HDAC3		NM_010411
Forward	5′-GCCTTCAACGTGGGTGATG-3′	
Reverse	5′-CCTGTGTAACGGGAGCAGAAC-3′	
Mouse HDAC4		NM_207225
Forward	5′-GATCCTCATTGTAGACTGGGATGTAC-3′	
Reverse	5′-ATAGCGGTGCAGGGACATGTA-3′	
Mouse HDAC6		NM_010413
Forward	5′-AAAAGAAGCACCGCATTCAGA-3′	
Reverse	5′-GTTCATATCGGTGGATGGAGAAA-3′	
Mouse HDAC7		NM_019572
Forward	5′-GACCCCAGTGTGCTCTACATTTC-3′	
Reverse	5′-TGCCAGTTCCCACCTCATC-3′	
Mouse collagen Ia		NM_007742
Forward	5′-GCCTTGGAGGAAACTTTGCTT-3′	
Reverse	5′-GCACGGAAACTCCAGCTGAT-3′	
Mouse α-SMA		NM_007392
Forward	5′-CACGGCATCATCACCAACTG-3′	
Reverse	5′-GGCCACACGAAGCTCGTTAT-3′	
Mouse CSF-1		NM_007778
Forward	5′-GGGGTGGAAGACATTCTTGA-3′	
Reverse	5′-TGTCAGTCTCTGCCTGGATG-3′	
Mouse EMR-1		NM_010130
Forward	5′-TGGCTGCCTCCCTGACTTT-3′	
Reverse	5′-ATTGCTGTATCTGCTCACTTTGGA-3′	
Mouse MCP-1		NM_011333
Forward	5′-GCAGTTAACGCCCCACTCA-3′	
Reverse	5′-CCTACTCATTGGGATCATCTTGCT-3′	
Rat CSF-1		NM_023981
Forward	5′-CATCCAGGCAGAGACTGACA-3′	
Reverse	5′-TGTCAACGGGGTGTCTGTTA-3′	
Rat HDAC1		XM_576595
Forward	5′-AATTTGCTGCTCAACTATGGTCTCT-3′	
Reverse	5′-TGATGTAGTCGTCGCTGTGGTACT-3′	
Rat HDAC2		XM_342149
Forward	5′-CCATGGCGTACAGTCAAGGA-3′	
Reverse	5′-AATAATTCCCGATATCACCGTCATA-3′	

HDAC, histone deacetylase; SMA, smooth muscle actin; CSF-1, colony-stimulating factor 1; EMR-1, epidermal growth factor-like molecule containing mucin-like hormone receptor 1; MCP-1, monocyte chemoattractant protein 1.

coronal sections of renal tissue were immersion-fixed in 10% neutral-buffered formalin and embedded in paraffin. The right kidneys from the same mice were examined as samples of kidneys not subjected to injury. Animal care and treatment complied with the standards described in the Guidelines for the Care and Use of Laboratory Animals of the University of Tokyo.

Renal morphology. To investigate morphological changes, 4-μm paraffin sections were stained by the Masson's trichrome method and examined by light microscopy. Images were obtained with a digital camera (DXM 1200C, Nikon, Tokyo, Japan). Interstitial fibrosis was scored semiquantitatively as previously reported (9) and graded as follows: 0, no staining; 1+, mild staining; 2+, moderate staining; 3+, marked staining; and 4+, severe staining. At least 10 different cortical fields (×200) were randomly selected from each specimen by one of the authors, who was unaware of the origin of the slides.

Immunohistochemistry. For the immunohistochemical staining of HDAC1, HDAC2, acetylated histone H3, and F4/80, a marker of macrophages which is also designated epidermal growth factor-like molecule containing mucin-like hormone receptor 1 (EMR-1), in the renal tissue, coronal sections of the renal tissue were immersion-fixed in 4% buffered-paraformaldehyde for 12 h, washed with 10, 15, and 20% sucrose in PBS for 4 h each time, embedded in Optimal Cutting Temperature compound, and snap-frozen in liquid nitrogen. Frozen sections, 6 μm in thickness, were stained with rabbit anti-HDAC1 polyclonal antibody (dilution 1:100, Lab Vision Products, Thermo Fisher Scientific, Fremont, CA), rabbit anti-HDAC2 polyclonal antibody (dilution 1:50, Santa Cruz Biotechnology, Santa Cruz, CA), rabbit anti-acetylated histone H3 (Lys9) polyclonal antibody (dilution 1:300, Upstate Biotechnology), and rat anti-F4/80 monoclonal antibody (dilution 1:100, Serotec, Oxford, UK), as the respective primary antibodies. For HDAC1, HDAC2, and acetylated histone H3, Alexa Fluor 488 goat anti-rabbit IgG (Molecular Probes, Eugene, OR) was used as the secondary antibody at a dilution of 1:200. Slides were mounted with Vectashield antifade mounting medium with DAPI

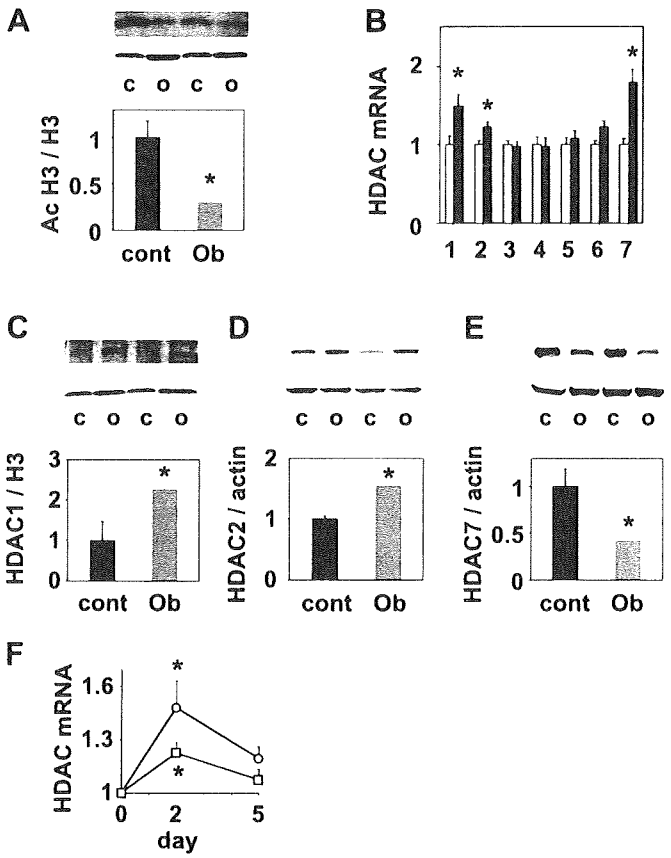

Fig. 1. Decrease in histone acetylation and induction of histone deacetylase (HDAC) 1 and HDAC2 by unilateral ureteral obstruction (UUO) for 2 days. *A*: representative films of Western blot analysis for acetylated histone and actin obtained from contralateral (c or cont) and obstructed (o or Ob) kidneys (*top* and *middle*, respectively). The results of densitometric analysis are shown at the *bottom*. Values are means ± SE (n = 5). *P < 0.05 vs. values of contralateral kidneys. *B*: changes in the mRNA levels of HDAC isozymes determined by RT-PCR are shown. Values of contralateral (open bars) and obstructed (filled bars) kidneys were normalized to those for 18S and expressed as relative values of contralateral kidneys. Values are means ± SE (n = 4–8). *P < 0.05 vs. values of contralateral kidneys. *C–E*: representative films of Western blot analysis for HDAC1 (*C*), HDAC2 (*D*), and HDAC7 (*E*) obtained from contralateral (c or cont) and obstructed (o or Ob) kidneys are shown (*top*). Blots for histone H3 (*C*) and actin (*D* and *E*) are also shown (*middle*). The results of densitometric analysis are shown at the *bottom*. Values are means ± SE (n = 4–5). *P < 0.05 vs. values of contralateral kidneys. *F*: time course of increase in HDAC. HDAC1 (○) and HDAC2 (□) mRNA levels of obstructed kidneys were normalized to values for 18S and expressed as relative values of contralateral kidneys. Values are means ± SE (n = 4–8). *P < 0.05 vs. values of contralateral kidneys.

表 3 Comparison of epidemiology of ANCA-associated renal vasculitis in Japan and UK

	Japan(Miyazaki)	UK(Norwich)
Male : Female	24 : 32	13 : 14
Mean age(yr)	70.4	63.5
Incidence(/million)		
Total	14.8(10.8～18.9)	12.2(8.0～17.7)
MPA/RLV	14.8(10.8～17.9)	4.9(2.4～8.8)
WG	0	5.8(2.9～9.4)
CSS	0	1.4(0.3～3.9)

例(95 %CI 33.2-56.3)の発症率であった[13]。この数値は，英国 Bristol(12.4 例)[14]，Norfolk(18 例，95 %CI 13-24)[15]，スウェーデン Orebro(16 例，95 %CI 12-31)[16]の腎血管炎の発症率と大差はなかった。

本邦の ANCA 関連腎血管炎の特徴

ANCA 関連腎血管炎に関して，宮崎県の retrospective study と同じ診断基準で，同じ 5 年間に英国 Norwich で行われた prospective study の結果を比較検討した。**表 3** に示すように，宮崎では全例が MPA であったが，Norwich では WG，MPA，CSS(各々の年間発症数は 5.8，4.9，1.4 例/100 万人)が含まれており，両国間で ANCA 関連腎血管炎の発症率はほぼ同等であるにもかかわらず，疾患内容が異なることが明らかとなった。また，臨床症状も異なり，特に ENT 所見では 1.8 % vs. 66.7 %と大差を認めた。さらに，宮崎と Norwich では ANCA の種類も異なっており，MPO-ANCA がそれぞれ 91.1 % vs. 55.6 %，PR3-ANCA が 0 % vs. 33.3 %であった(**表 4**)[17]。この結果は，本邦の RPGN(主に pauci-immune 型半月体形成性糸球体腎炎)や MPA/RLV の 80～90 %は MPO-ANCA が陽性であるのに対し，欧米では PR3-ANCA の陽性例が 25～35 %程度にみられるという今までの報告[10～12,16,18～20](**表 5**)を裏付けるものであった。

しかしながら，宮崎の調査が nephrologists により行われたのに対し，Norwich では rheumatologists によるものであった。そこで，宮崎ではその後の 4 年間(2005～2008 年)，rheumatologists の参画も得て同じ調査を毎年行っている。この間に登録された 61 症例のなかに WG と CSS による ANCA 関連腎血管炎を各々 3 症例，PR3-ANCA 陽性例を 3 例認めたが，①WG は本邦では稀，②MPO-/PR3-ANCA 比は欧米に比べて明らかに本邦で高い，ことが再確認されている。

表 4 Comparison of clinical features of ANCA-associated renal vasculitis in Japan and UK

	Japan(Miyazaki)	UK(Norwich)	
ENT	1(1.8 %)	18(66.7 %)	p<0.001
Respiratory	23(41.1 %)	11(40.7 %)	ns
Nervous	3(5.4 %)	8(29.6 %)	p<0.02
Gastrointestinal	2(3.6 %)	3(11.1 %)	ns
MPO-ANCA	51(91.1 %)	15(55.6 %)	p<0.001
PR3-ANCA	0(0.0 %)	9(33.3 %)	p<0.001
Negative ANCA	5(8.9 %)	2(7.4 %)	ns

ENT : ear, nose, and throat

表 5 Difference in ANCA phenotype in patients with pauci-immune crescentic glomerulonephritis/microscopic polyangiitis/renal limited vasculitis between Japan and foreign countries

Country [reference number]	Patients number	Positive MPO-ANCA	Positive PR3-ANCA
USA[18]	107	64 %	36 %
EU[19]	80	63 %	25 %
Sweden[16]	99	48 %	32 %
UK[20]	153	65 %	25 %
Japan[10]	63	79 %	13 %
Japan[11]	369	90 %	8 %
Japan[12]	993	89 %	6 %

ANCA 関連血管炎の本邦と欧米の差異の原因

本邦で MPO-ANCA 陽性の RPGN あるいは血管炎が多い原因として，本邦では高齢患者が多いこと以外に，遺伝的な背景[21,22]，環境因子[23,24]，緯度の差異[10,13]などが疑われている。表 1 に示したように，欧州では北では WG，南では MPA が多いことが知られており，緯度の低い宮崎で WG が非常に少ないことと関連しているのかもしれない。なお，MPO-/PR3-ANCA 比が本邦と欧州で異なる原因が測定試薬キットに起因するものではないことは明らかにされている[25]。

おわりに

ANCA 関連血管炎の疫学が，本邦と欧米とでは異なることが明らかとなってきた。このことは，厚生労働省進行性腎障害研究班の RPGN 分科会が指摘しているように，本邦特有の治療法確立の重要性に繋がっているとも考えられる。一方，新しい血管炎の定義，分類基準，診断基準が統

histochemical stainings were obtained by substitution of the primary antibody with PBS or normal IgG.

Western blotting. Renal tissue was immediately snap-frozen in liquid nitrogen and stored at −70°C and further processed according to a previously described method (6, 13). After determination of the protein concentrations of the lysates with a protein assay kit (Bio-Rad, Richmond, CA), equal amounts of protein (100 μg) were immunoblotted with rabbit anti-acetyl histone H3 (Lys9) polyclonal antibody (Upstate Biotechnology), HDAC1 (Sigma), HDAC2 (Santa Cruz Biotechnology), HDAC7 (Sigma), or α-SMA (Dako) and analyzed using standard SDS-PAGE and Western blotting (22). For the detection of HDAC1, the nuclear protein was used to reduce nonspecific bands observed in blots using the whole tissue extract. The nuclear protein was extracted using a Nuclear/Cytosol Fraction Kit (BioVision Research Products, Mountain View, CA) in accordance with the manufacturer's instructions. β-Actin (41) and H3 (23, 27) were used as the loading controls for whole cell lysate and nuclear protein, respectively. The values obtained by densitometric analysis of Western blots were normalized to those for actin or histone H3 and expressed as relative values to those of control.

Analysis of mRNA levels. Total RNA was extracted from renal tissue or NRK 52E with an RNA extraction kit, RNeasy Mini (Qiagen, Tokyo, Japan). The cDNA product was generated using a high-capacity cDNA archive kit (Applied Biosystems, Foster City, CA). The expression levels of HDAC isozymes, collagen 1a, α-SMA, EMR-1, MCP-1, and CSF-1 were analyzed with the ABI 7500 sequence detection system using SYBR Green PCR Master Mix (Applied Biosystems). Primer sequences are shown in Table 1. For detection of mouse HDAC5 and 18S ribosomal RNA, primers and probes were obtained from Applied Biosystems, and Taqman Universal PCR Master Mix was used. The thermal cycling parameters were 95°C for 10 min for AmpliTaq Gold activation, followed by 40 cycles of 15 s at 95°C for denaturation, and 1 min at 60°C for annealing/extension. Values were normalized to the

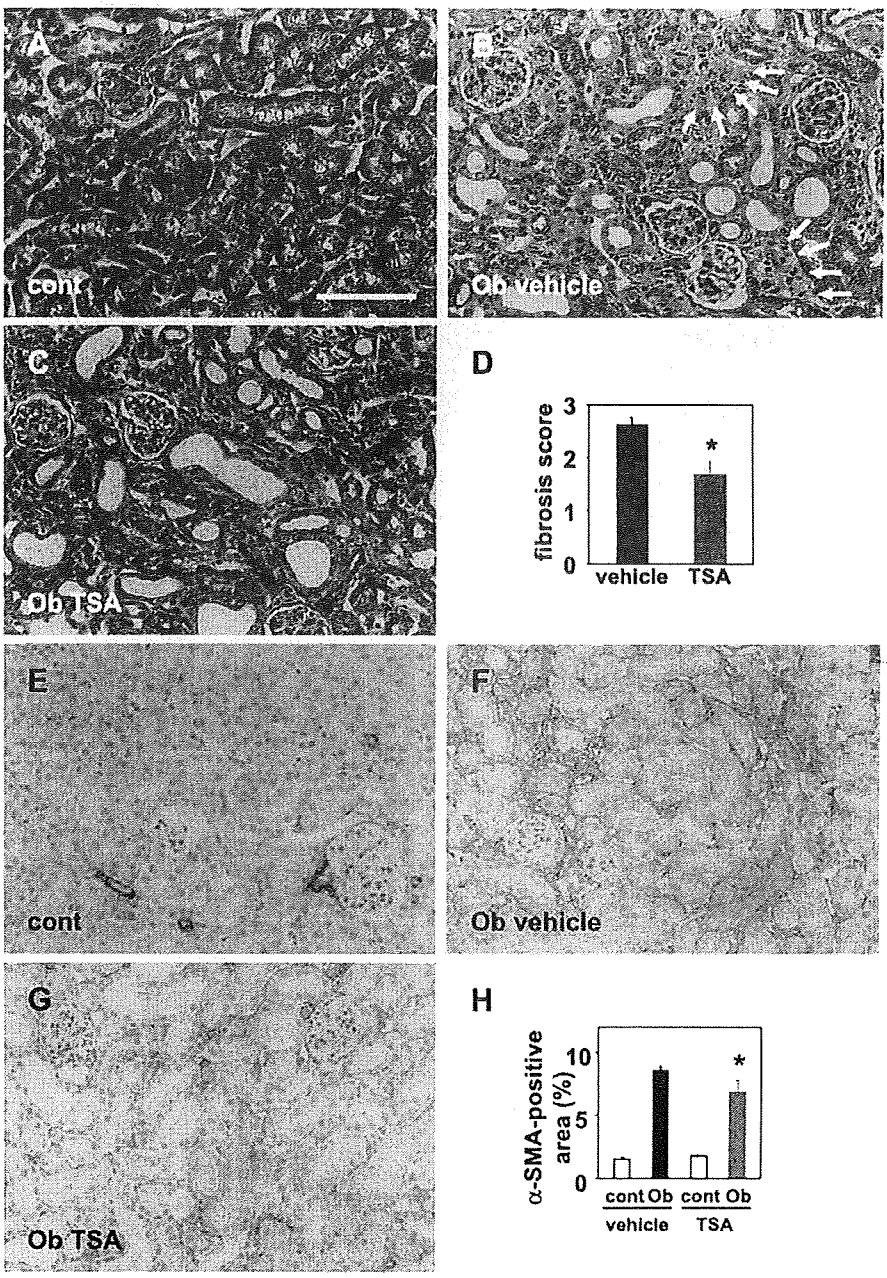

Fig. 3. Attenuation of tubulointerstitial fibrosis in UUO mice by HDAC inhibition. Representative photomicrographs of Masson's trichrome staining (*A–C*) and α-smooth muscle action (SMA) staining (*E–G*) of the contralateral (*A* and *E*) and injured (*B*, *C*, *F*, and *G*) kidneys. The UUO mice received intraperitoneal injections of vehicle (*A*, *B*, *E*, and *F*) or trichostatin A (TSA; *C* and *G*). Kidney sections were obtained 5 days after ureteral obstruction. Expansion of interstitial space by extracellular matrix and inflammatory cells observed in *B* (arrows) was reduced (*C*). Values are means ± SE of the average interstitial fibrosis score and α-SMA-positive area, respectively, from 5 mice that had received the intraperitoneal injections of vehicle or TSA. Bar = 100 μm. *$P < 0.05$ vs. values of obstructed kidneys obtained from mice treated with vehicle.

20. **Lenda DM, Kikawada E, Stanley ER, Kelley VR.** Reduced macrophage recruitment, proliferation, and activation in colony-stimulating factor-1-deficient mice results in decreased tubular apoptosis during renal inflammation. *J Immunol* 170: 3254–3262, 2003.
21. **Marumo T, Hishikawa K, Yoshikawa M, Fujita T.** Epigenetic regulation of BMP7 in the regenerative response to ischemia. *J Am Soc Nephrol* 19: 1311–1320, 2008.
22. **Marumo T, Uchimura H, Hayashi M, Hishikawa K, Fujita T.** Aldosterone impairs bone marrow-derived progenitor cell formation. *Hypertension* 48: 490–496, 2006.
23. **Mathew S, Tustison KS, Sugatani T, Chaudhary LR, Rifas L, Hruska KA.** The mechanism of phosphorus as a cardiovascular risk factor in CKD. *J Am Soc Nephrol* 19: 1092–1105, 2008.
24. **Mejat A, Ramond F, Bassel-Duby R, Khochbin S, Olson EN, Schaeffer L.** Histone deacetylase 9 couples neuronal activity to muscle chromatin acetylation and gene expression. *Nat Neurosci* 8: 313–321, 2005.
25. **Minetti GC, Colussi C, Adami R, Serra C, Mozzetta C, Parente V, Fortuni S, Straino S, Sampaolesi M, Di Padova M, Illi B, Gallinari P, Steinkuhler C, Capogrossi MC, Sartorelli V, Bottinelli R, Gaetano C, Puri PL.** Functional and morphological recovery of dystrophic muscles in mice treated with deacetylase inhibitors. *Nat Med* 12: 1147–1150, 2006.
26. **Mishra N, Reilly CM, Brown DR, Ruiz P, Gilkeson GS.** Histone deacetylase inhibitors modulate renal disease in the MRL-lpr/lpr mouse. *J Clin Invest* 111: 539–552, 2003.
27. **Montgomery RL, Potthoff MJ, Haberland M, Qi X, Matsuzaki S, Humphries KM, Richardson JA, Bassel-Duby R, Oslon EN.** Maintenance of cardiac energy metabolism by histone deacetylase 3 in mice. *J Clin Invest* 118: 3588–3597, 2008.
28. **Nott A, Watson PM, Robinson JD, Crepaldi L, Riccio A.** S-nitrosylation of histone deacetylase 2 induces chromatin remodelling in neurons. *Nature* 455: 411–415, 2008.
29. **Pandey UB, Nie Z, Batlevi Y, McCray BA, Ritson GP, Nedelsky NB, Schwartz SL, DiProspero NA, Knight MA, Schuldiner O, Padmanabhan R, Hild M, Berry DL, Garza D, Hubbert CC, Yao TP, Baehrecke EH, Taylor JP.** HDAC6 rescues neurodegeneration and provides an essential link between autophagy and the UPS. *Nature* 447: 859–863, 2007.
30. **Reddy P, Sun Y, Toubai T, Duran-Struuck R, Clouthier SG, Weisiger E, Maeda Y, Tawara I, Krijanovski O, Gatza E, Liu C, Malter C, Mascagni P, Dinarello CA, Ferrara JL.** Histone deacetylase inhibition modulates indoleamine 2,3-dioxygenase-dependent DC functions and regulates experimental graft-versus-host disease in mice. *J Clin Invest* 118: 2562–2573, 2008.
31. **Ricardo SD, van Goor H, Eddy AA.** Macrophage diversity in renal injury and repair. *J Clin Invest* 118: 3522–3530, 2008.
32. **Sakamoto S, Potla R, Larner AC.** Histone deacetylase activity is required to recruit RNA polymerase II to the promoters of selected interferon-stimulated early response genes. *J Biol Chem* 279: 40362–40367, 2004.
33. **Seligson DB, Horvath S, Shi T, Yu H, Tze S, Grunstein M, Kurdistani SK.** Global histone modification patterns predict risk of prostate cancer recurrence. *Nature* 435: 1262–1266, 2005.
34. **Tang H, Macpherson P, Marvin M, Meadows E, Klein WH, Yang XJ, Goldman D.** A histone deacetylase 4/myogenin positive feedback loop coordinates denervation-dependent gene induction and suppression. *Mol Biol Cell* 20: 1120–1131, 2009.
35. **Tao R, de Zoeten EF, Ozkaynak E, Chen C, Wang L, Porrett PM, Li B, Turka LA, Olson EN, Greene MI, Wells AD, Hancock WW.** Deacetylase inhibition promotes the generation and function of regulatory T cells. *Nat Med* 13: 1299–1307, 2007.
36. **Trivedi CM, Luo Y, Yin Z, Zhang M, Zhu W, Wang T, Floss T, Goettlicher M, Noppinger PR, Wurst W, Ferrari VA, Abrams CS, Gruber PJ, Epstein JA.** Hdac2 regulates the cardiac hypertrophic response by modulating Gsk3beta activity. *Nat Med* 13: 324–331, 2007.
37. **Uchimura H, Marumo T, Takase O, Kawachi H, Shimizu F, Hayashi M, Saruta T, Hishikawa K, Fujita T.** Intrarenal injection of bone marrow-derived angiogenic cells reduces endothelial injury and mesangial cell activation in experimental glomerulonephritis. *J Am Soc Nephrol* 16: 997–1004, 2005.
38. **Urbich C, Rossig L, Kaluza D, Potente M, Boeckel JN, Knau A, Diehl F, Geng JG, Hofmann WK, Zeiher AM, Dimmeler S.** HDAC5 is a repressor of angiogenesis and determines the angiogenic gene expression pattern of endothelial cells. *Blood* 113: 5669–5679, 2009.
39. **Xu WS, Parmigiani RB, Marks PA.** Histone deacetylase inhibitors: molecular mechanisms of action. *Oncogene* 26: 5541–5552, 2007.
40. **Yamaguchi K, Lantowski A, Dannenberg AJ, Subbaramaiah K.** Histone deacetylase inhibitors suppress the induction of c-Jun and its target genes including COX-2. *J Biol Chem* 280: 32569–32577, 2005.
41. **Yang J, Shultz RW, Mars WM, Wegner RE, Li Y, Dai C, Nejak K, Liu Y.** Disruption of tissue-type plasminogen activator gene in mice reduces renal interstitial fibrosis in obstructive nephropathy. *J Clin Invest* 110: 1525–1538, 2002.
42. **Yoshikawa M, Hishikawa K, Marumo T, Fujita T.** Inhibition of histone deacetylase activity suppresses epithelial-to-mesenchymal transition induced by TGF-beta1 in human renal epithelial cells. *J Am Soc Nephrol* 18: 58–65, 2007.

ment indeed increased the level of histone acetylation of renal tubular cells, as judged from the observation that while there were some tubular cells negative for histone acetylation staining in obstructed kidneys obtained from mice treated with vehicle (Fig. 5, *A* and *B*, arrowheads), most of the tubular cells in the obstructed kidneys obtained from mice treated with TSA were positive for acetylated histone (Fig. 5, *C* and *D*). Tubular cells positive for nuclear staining with acetylated histone was significantly increased in TSA-treated animals (Fig. 5*E*).

HDAC inhibitor attenuates inflammation. We next examined the effects of HDAC inhibition on the macrophage infiltration and chemokine expression induced by UUO. Macrophage infiltration and the increase in mRNA levels of EMR-1 (F4/80), a marker of macrophages, were significantly reduced in the obstructed kidneys obtained from mice treated with TSA compared with those in kidneys obtained from mice treated with vehicle (Fig. 6, *A* and *B*). Since MCP-1 and CSF-1 have been shown to mediate macrophage infiltration in the early phase of UUO (2, 16, 19, 20), we determined the effects of HDAC inhibitor on the mRNA levels of these chemokines. While the induction of MCP-1 mRNA was not altered, the increase in the level of CSF-1 mRNA was significantly lower in the obstructed kidneys of TSA-treated mice than in those of mice treated with vehicle (Fig. 6, *C* and *D*). These results suggest that TSA may attenuate inflammation, at least in part, by inhibiting induction of CSF-1 but not MCP-1.

Involvement of HDAC1 and HDAC2 in CSF-1 expression in tubular cells. To gain further insight into the role of HDAC in CSF-1 induction, we next used rat tubular epithelial cells (NRK 52E). Stimulation of the tubular cells with TNF-α, a cytokine involved in renal injury induced by UUO (5), significantly induced CSF-1 mRNA (Fig. 7*A*). In accordance with the results obtained in UUO, TSA attenuated the induction of CSF-1 (Fig. 7*A*), while it had no effects on MCP-1 induction (Fig. 7*B*). Valproate, another HDAC inhibitor, also reduced CSF-1 induction by TNF-α (Fig. 7*C*). These results indicate that HDAC indeed plays a critical role in CSF-1 induction in renal tubular cells. To delineate the possible roles of HDAC1 and HDAC2 on CSF-1 induction, we knocked down the expression of HDACs using RNA interference (RNAi). The HDAC1 mRNA level was markedly reduced following the transfection of HDAC1 Stealth RNAi, compared with that of cells transfected with control Stealth RNAi [HDAC1 Stealth RNAi (0.16 ± 0.01 arbitrary units) vs. control Stealth RNAi (1.00 ± 0.20 arbitrary units; $P < 0.05$; $n = 8$)]. The induction of CSF-1 by TNF-α was prevented by the downregulation of HDAC1 (Fig. 7*D*). The knockdown of HDAC2 by HDAC2 Stealth RNAi [HDAC2 Stealth RNAi (0.10 ± 0.01 arbitrary units) vs. control Stealth RNAi (1.00 ± 0.17 arbitrary units, $P < 0.05$, $n = 8$)] also reduced CSF-1 induction by TNF-α, although the reduction in CSF-1 mRNA was less pronounced than that achieved by HDAC1 knockdown (Fig. 7*E*). These results indicate the important roles of HDAC1 and HDAC2 in the expression of CSF-1 in tubular cells stimulated with TNF-α.

DISCUSSION

Accumulating evidence indicates that the changes in HDAC expression and histone acetylation are involved in transmission

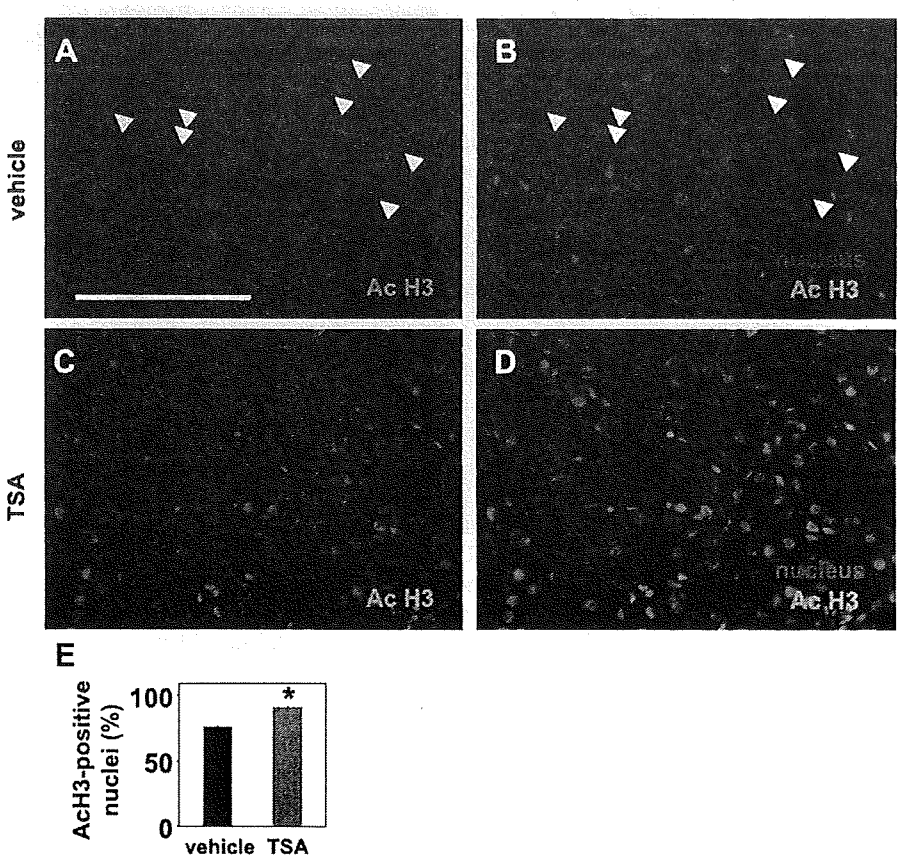

Fig. 5. Representative photomicrographs of staining with acetylated histone of the injured kidneys obtained from mice treated with vehicle (*A* and *B*) or TSA (*C* and *D*). Samples were obtained on *day 2*. Localization of nuclei in the same sections (*A* and *C*) is shown by costaining with DAPI (red) in *B* and *D*, respectively. Nuclei stained negative for acetylated histone are shown by arrowheads in *A* and *B*. *E*: quantitative analysis of tubular cells positive for acetylated histone in the injured kidneys obtained from mice treated with vehicle or TSA. Values are means ± SE expressed as a percentage of total nuclei ($n = 5$). Bar = 100 μm.*$P < 0.05$ vs. values of obstructed kidneys obtained from mice treated with vehicle.

(Vector Laboratories, Burlingame, CA). Images were obtained with a digital camera (DXM 1200C, Nikon) attached to an Eclipse E600 epifluorescence microscope (Nikon). For determination of the percentage of cells positive for acetylated histone, HDAC1, and HDAC2, at least eight different fields in the cortex of each kidney, each containing at least 50 proximal tubular cells, were analyzed. For the detection of F4/80, immobilized antibody was detected using the biotin-avidin-immunoperoxidase technique with a Vectastain ELIT ABC kit (Vector Laboratories) and 3–3′-diaminobenzidine as the chromogen. Sections were then counterstained with Mayer's hematoxylin and examined by light microscopy. The number of F4/80-positive cells in the cortical area was counted in a blinded fashion in at least 10 different cortical fields (×200) for each section, and the mean values per section were calculated. For the detection of α-SMA, deparaffinized sections, 4 μm thick, were stained with mouse anti-α-SMA monoclonal antibody (1:50 dilution, 1A4, Dako), according to a method previously described (37). Immobilized antibody was detected using the biotin-avidin-immunoperoxidase technique with a Vectastain ELIT ABC kit (Vector Laboratories) and 3–3′-diaminobenzidine as the chromogen. Sections were then counterstained with Mayer's hematoxylin and examined by light microscopy. The ratio of the interstitial α-SMA-positive area to the cortical area was calculated by image analysis using a Nikon ACT-1C, Adobe Photoshop 7.0, and Scion Image. The mean value of the α-SMA-positive area was obtained by evaluating at least 10 different cortical fields (×200) from each kidney in a blinded manner. Negative controls for all the immuno-

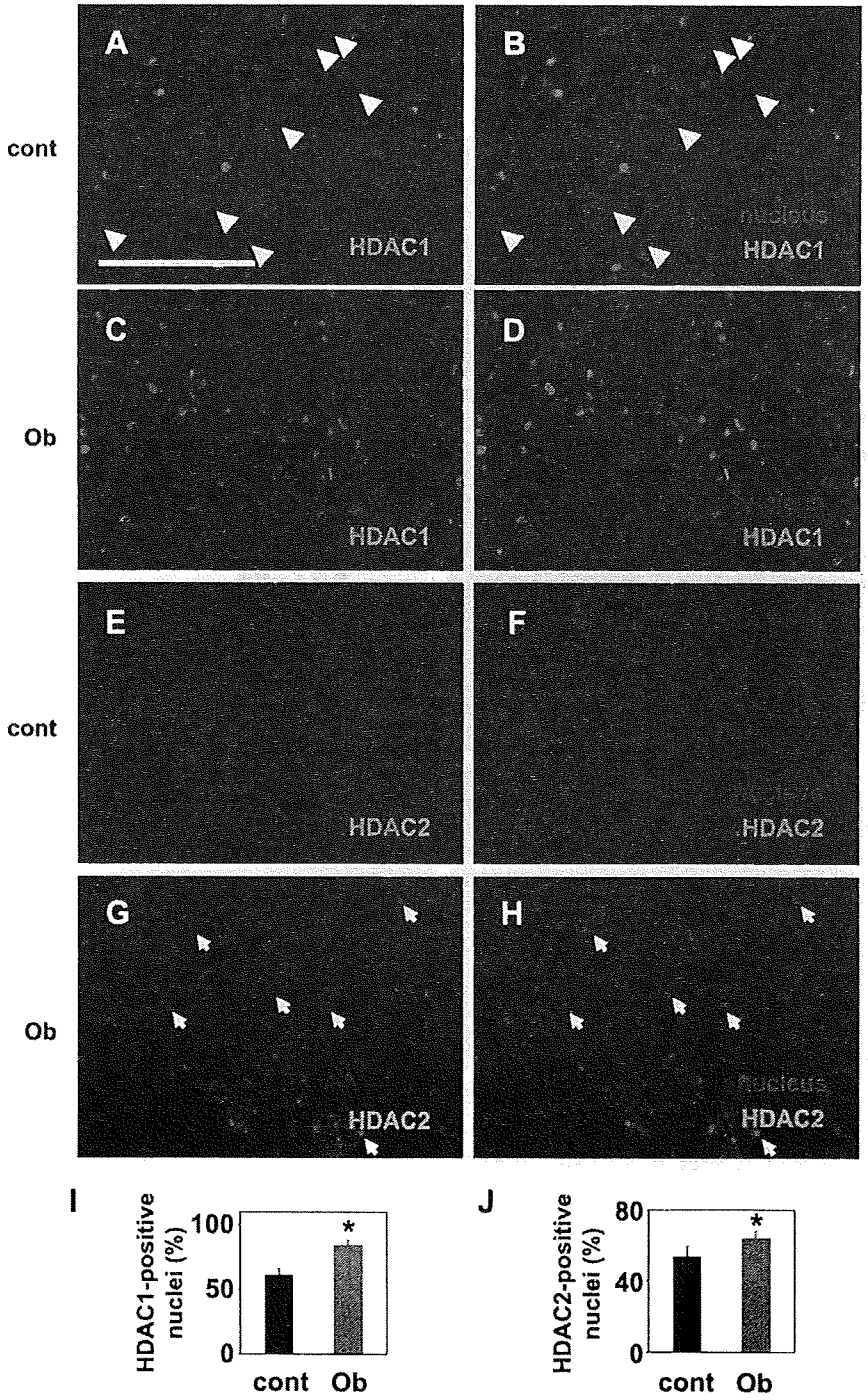

Fig. 2. Increase in tubular expression of HDAC1 and HDAC2 by UUO. Immunohistochemical staining of the renal cortex from contralateral (*A*, *B*, *E*, and *F*) and obstructed (*C*, *D*, *G*, and *H*) kidneys with HDAC1 (*A–D*) and HDAC2 (*E–H*) at 2 days after obstruction is shown in green. Localization of nuclei in the same sections (*A*, *C*, *E*, and *G*) is shown by costaining with DAPI (red) in panels *B*, *D*, *F*, and *H*, respectively. Bar = 100 μm. Nuclei stained negative for HDAC1 are shown by arrowheads in *A* and *B*. Nuclei stained positive for HDAC2 are shown by arrows in *G* and *H*. Quantitative analysis of nuclei positive for HDAC1 (*I*) and HDAC2 (*J*) in the cortex of contralateral and obstructed kidneys is shown. Values are means ± SE expressed as a percentage of total nuclei (n = 4–5). *P < 0.05 vs. values of contralateral kidneys.

stage of injury mediates resolution of inflammation, the initial phase of macrophage infiltration has been regarded to promote renal fibrosis (1, 2, 8, 19). In addition, the inhibition of epithelial-to-mesenchymal transition by HDAC inhibition (42) may also be involved in reduced fibrosis by TSA to some extent, since a considerable amount of myofibroblasts have been shown to be derived from renal tubular cells by the epithelial-to-mesenchymal transition in UUO-induced fibrotic changes (15).

Although acetylated histones are generally associated with active gene transcription, HDAC inhibition attenuated mRNA levels of CSF-1. The mechanism remains to be elucidated, but we can speculate about some possibilities. For example, HDAC inhibition may lead to an increase in a factor which exerts an inhibitory effect on CSF-1 transcription. It is also possible that HDAC inhibition may reduce recruitment of transcription factors or RNA polymerase II to the CSF-1 promoter, as has been reported for molecules such as c-jun (40) or interferon-stimulated immediate early genes (32).

CSF-1 induction was only partially inhibited by TSA in the present study. However, HDAC activity in nuclear extracts of NRK 52E cells was almost completely inhibited in the presence of 100 nM TSA (data not shown). These results suggest that HDAC may not be the sole activator of the CSF-1 increase under these conditions.

More than 10 HDAC inhibitors have already been examined in clinical trials as antitumor agents with only minor side effects observed (39). In addition to antitumor activities, HDAC inhibitors have been shown to exert beneficial effects on several diseases such as cardiac hypertrophy (4, 18), neuromuscular diseases (3, 10, 25), and inflammatory bowel disease (35). In line with these reports, we and others reported the beneficial effects of HDAC inhibition on glomerular diseases (13, 26). The present study suggests that HDAC inhibitor may also be useful for treatment of tubulointerstitial injury, at least in the early stage. By using the UUO model, the present study clarified that HDAC inhibition reduces tubulointerstitial lesions via a direct mechanism in the tubulointerstitial region independently of glomerular lesions or proteinuria. The precise mechanisms of the renoprotective effects of HDAC inhibitor, especially the target HDAC isozyme, needs to be clarified, considering that different HDAC isozymes can exert even opposite effects under some conditions such as hypertrophy of the heart (4, 36) and angiogenesis (7, 38). In this regard, the present study revealed that HDAC1 and HDAC2, which are increased in injured tubular cells, can act as targets of HDAC inhibitors for reducing CSF-1 expression and inflammation in tubulointerstitial injury.

In conclusion, the present study reveals that HDAC1 and HDAC2 are induced in renal tubular cells in response to tubulointerstitial injury. Increased HDAC1 and HDAC2 in tubular cells are likely to contribute to the expression of CSF-1 and the subsequent inflammatory process. These findings reveal the unrecognized role of HDAC changes in the initiation of tubulointerstitial injury and suggest HDAC inhibition as a potential therapeutic strategy for the treatment of inflammation and fibrosis in the early stage of tubulointerstitial injury.

GRANTS

This work was supported by Mochida Pharmaceutical, Co., Ltd., the Takeda Science Foundation, a Grant-in-Aid for Scientific Research from the Japan Society for the Promotion of Science, and a grant from the Ministry of Health, Labour and Welfare.

DISCLOSURES

No conflicts of interest are declared by the authors.

REFERENCES

1. **Abbate M, Zoja C, Remuzzi G.** How does proteinuria cause progressive renal damage? *J Am Soc Nephrol* 17: 2974–2984, 2006.
2. **Anders HJ, Vielhauer V, Frink M, Linde Y, Cohen CD, Blattner SM, Kretzler M, Strutz F, Mack M, Grone HJ, Onuffer J, Horuk R, Nelson PJ, Schlondorff D.** A chemokine receptor CCR-1 antagonist reduces renal fibrosis after unilateral ureter ligation. *J Clin Invest* 109: 251–259, 2002.
3. **Avila AM, Burnett BG, Taye AA, Gabanella F, Knight MA, Hartenstein P, Cizman Z, Di Prospero NA, Pellizzoni L, Fischbeck KH, Sumner CJ.** Trichostatin A increases SMN expression and survival in a mouse model of spinal muscular atrophy. *J Clin Invest* 117: 659–671, 2007.
4. **Backs J, Olson EN.** Control of cardiac growth by histone acetylation/deacetylation. *Circ Res* 98: 15–24, 2006.
5. **Bascands JL, Schanstra JP.** Obstructive nephropathy: insights from genetically engineered animals. *Kidney Int* 68: 925–937, 2005.
6. **Bokemeyer D, Panek D, Kramer HJ, Lindemann M, Kitahara M, Boor P, Kerjaschki D, Trzaskos JM, Floege J, Ostendorf T.** In vivo identification of the mitogen-activated protein kinase cascade as a central pathogenic pathway in experimental mesangioproliferative glomerulonephritis. *J Am Soc Nephrol* 13: 1473–1480, 2002.
7. **Chang S, Young BD, Li S, Qi X, Richardson JA, Olson EN.** Histone deacetylase 7 maintains vascular integrity by repressing matrix metalloproteinase 10. *Cell* 126: 321–334, 2006.
8. **Eardley KS, Cockwell P.** Macrophages and progressive tubulointerstitial disease. *Kidney Int* 68: 437–455, 2005.
9. **Esteban V, Lorenzo O, Ruperez M, Suzuki Y, Mezzano S, Blanco J, Kretzler M, Sugaya T, Egido J, Ruiz-Ortega M.** Angiotensin II, via AT1 and AT2 receptors and NF-kappaB pathway, regulates the inflammatory response in unilateral ureteral obstruction. *J Am Soc Nephrol* 15: 1514–1529, 2004.
10. **Fischer A, Sananbenesi F, Wang X, Dobbin M, Tsai LH.** Recovery of learning and memory is associated with chromatin remodelling. *Nature* 447: 178–182, 2007.
11. **Guan JS, Haggarty SJ, Giacometti E, Dannenberg JH, Joseph N, Gao J, Nieland TJ, Zhou Y, Wang X, Mazitschek R, Bradner JE, DePinho RA, Jaenisch R, Tsai LH.** HDAC2 negatively regulates memory formation and synaptic plasticity. *Nature* 459: 55–60, 2009.
12. **Haberland M, Montgomery RL, Olson EN.** The many roles of histone deacetylases in development and physiology: implications for disease and therapy. *Nat Rev Genet* 10: 32–42, 2009.
13. **Imai N, Hishikawa K, Marumo T, Hirahashi J, Inowa T, Matsuzaki Y, Okano H, Kitamura T, Salant D, Fujita T.** Inhibition of histone deacetylase activates side population cells in kidney and partially reverses chronic renal injury. *Stem Cells* 25: 2469–2475, 2007.
14. **Ito K, Ito M, Elliott WM, Cosio B, Caramori G, Kon OM, Barczyk A, Hayashi S, Adcock IM, Hogg JC, Barnes PJ.** Decreased histone deacetylase activity in chronic obstructive pulmonary disease. *N Engl J Med* 352: 1967–1976, 2005.
15. **Iwano M, Plieth D, Danoff TM, Xue C, Okada H, Neilson EG.** Evidence that fibroblasts derive from epithelium during tissue fibrosis. *J Clin Invest* 110: 341–350, 2002.
16. **Jang MH, Herber DM, Jiang X, Nandi S, Dai XM, Zeller G, Stanley ER, Kelley VR.** Distinct in vivo roles of colony-stimulating factor-1 isoforms in renal inflammation. *J Immunol* 177: 4055–4063, 2006.
17. **Kee HJ, Eom GH, Joung H, Shin S, Kim JR, Cho YK, Choe N, Sim BW, Jo D, Jeong MH, Kim KK, Seo JS, Kook H.** Activation of histone deacetylase 2 by inducible heat shock protein 70 in cardiac hypertrophy. *Circ Res* 103: 1259–1269, 2008.
18. **Kook H, Lepore JJ, Gitler AD, Lu MM, Wing-Man Yung W, Mackay J, Zhou R, Ferrari V, Gruber P, Epstein JA.** Cardiac hypertrophy and histone deacetylase-dependent transcriptional repression mediated by the atypical homeodomain protein Hop. *J Clin Invest* 112: 863–871, 2003.
19. **Lange-Sperandio B, Trautmann A, Eickelberg O, Jayachandran A, Oberle S, Schmidutz F, Rodenbeck B, Homme M, Horuk R, Schaefer F.** Leukocytes induce epithelial to mesenchymal transition after unilateral ureteral obstruction in neonatal mice. *Am J Pathol* 171: 861–871, 2007.

expressed and secreted), macrophage inflammatory protein-1α, macrophage inflammatory protein-1β, eotaxin, keratinocyte-derived chemokine, fibroblast growth factor basic, leukemia inhibitory factor, macrophage colony-stimulating factor, monokine induced by interferon-gamma, macrophage inflammatory protein-2, platelet-derived growth factor-BB, and vascular endothelial growth factor.

Analysis of Renal E-Selectin

E-selectin levels in kidney homogenates were measured by an E-selectin assay kit (R&D Systems). Protein concentrations were determined by the Lowry assay with the Bio-Rad DC protein assay dye reagent.

Measurement of Granulocyte Elastase Digests of Plasma Fibrinogen and Fibrin

To obtain plasma, blood sampled from the retroorbital plexus was collected into plastic tubes containing sodium citrate and centrifuged. Fibrin degradation products specifically degraded by granulocyte-elastase (e-XDP) were measured by the E-XDP Test (Mitsubishi Kagaku Iatron Co, Tokyo, Japan), which consists of Tris buffer (R1) and latex reagent (R2) containing IF-123–coated latex beads. IF-123 specifically recognizes e-XDP.[13] The latex agglutination assay was performed with the use of an automatic analyzer LPIA-NV7 (Mitsubishi Kagaku Iatron Co). The test sample in Tris-saline buffer was mixed in a reaction cuvette at 37°C. Latex reagent was added to this mixture, and the absorbance at 800 nm was measured every 15 seconds for 7 minutes. The V value (latex agglutination velocity) was defined as Δabsorbance at 800 nm/min. The rate of agglutination was expressed in terms of ΔA800/min as a function of the concentration of e-XDP.

Statistical Analysis

Results are expressed as mean±SEM for data resulting from in vivo analyses of mice. In all cases, an unpaired t test was used to compare 2 groups. $P<0.05$ was considered statistically significant.

The authors had full access to and take full responsibility for the integrity of the data. All authors have read and agree to the manuscript as written.

Results

Development of a Murine Model of TGN

TGN was induced by the injection of lipopolysaccharide and anti-GBM serum (nephrotoxic serum), which reproducibly produced severe glomerular thrombosis within 72 hours (Figure 1A). Glomerular neutrophil accumulation was prominent and occurred as early as 4 hours after disease induction, whereas inflammatory cell infiltration into the tubulointerstitial area and fibrosis were minimal (data not shown). Glomerular crescent formation and sclerosis were absent, although tubular damage was observed, as characterized by tubular dilation and casts. This was associated with rapidly progressive renal failure, as evidenced by a significant elevation of serum creatinine and BUN (Figure 1B). Replacement of nephrotoxic serum with normal rabbit serum failed to induce TGN, suggesting that a combination of anti-GBM serum and lipopolysaccharide is required for disease induction (Figure 1A and 1B). The observed histopathological changes and renal dysfunction were also dependent on lipopolysaccharide, as anti-GBM antibody alone resulted only in acute neutrophil accumulation and mild proteinuira[14] (data not shown). Thus, lipopolysaccharide and in situ glomerular antibody deposits together trigger TGN.

To examine the contribution of neutrophils to TGN, neutrophils were immunodepleted with anti-Gr-1 monoclonal antibody 24 hours before disease induction (13.3±6.0 versus 548.8±196.4 neutrophils per microliter for Gr-1 monoclonal antibody [n=4] and control [n=4] groups, respectively, 24 hours after treatment). Neutrophil-depleted mice exhibited a marked reduction in glomerular thrombosis that correlated with significantly reduced indices of renal failure. These data suggest a primary role for neutrophils in the initiation of TGN (Figure 1C and 1D).

Mac-1 Is Essential for the Development of TGN

Mac-$1^{-/-}$ and WT cohorts were subjected to TGN. Mac-$1^{-/-}$ mice had minimal glomerular thrombosis and significantly reduced fibrin deposition (Figure 2A). The integrity of the glomerular microvasculature, a primary site of injury in microangiopathic disorders in humans, was evaluated by examining CD34, a marker of capillary endothelial cells that is transcriptionally downregulated in inflammatory settings.[15,16] Immunohistochemically, TGN led to a significant reduction of CD34 in the glomerular capillaries of WT mice, which is the primary site of injury in this model, whereas its expression in the interstitium was similar to that in untreated mice. In contrast, CD34 remained intact in Mac-$1^{-/-}$ mice subjected to TGN (Figure 2B). In addition, the cytokine-inducible, endothelial-specific adhesion molecule E-selectin was elevated in the renal tissue of WT mice, indicating endothelial activation, whereas this was much less pronounced in Mac-$1^{-/-}$ animals (Figure 2C). Together these data indicate a requirement for Mac-1 in endothelial activation and damage after TGN. Indices of renal dysfunction were significantly less pronounced in Mac-$1^{-/-}$ versus WT animals. Hematuria, a marker of hemorrhage, was milder in Mac-$1^{-/-}$ mice compared with WT counterparts (Figure 2D), and Mac-$1^{-/-}$ mice were resistant to TGN-induced renal failure, as evidenced by a significant attenuation in the elevation of serum creatinine, BUN, and LDH (Figure 2E). The protection from TGN in Mac-$1^{-/-}$ mice was associated with a marked reduction in glomerular neutrophil accumulation at both 4 and 24 hours after disease induction (Figure 2F). To assess whether changes in renal cytokine levels contribute to the observed protection in Mac-$1^{-/-}$ mice, multiplex cytokine analysis of renal tissue 4 hours after induction of TGN was conducted. Among 32 cytokines/chemokines measured, 16 were induced, and these were comparable in WT and Mac-$1^{-/-}$ mice (Table 1).

Hematologic abnormalities associated with TGN were less severe in Mac-$1^{-/-}$ mice. Mac-1 deficiency led to a partial attenuation of the observed thrombocytopenia in WT mice that likely reflects less platelet consumption. Mild anemia was present in both WT and Mac-$1^{-/-}$ mice, suggesting that it is not a consequence or predictor of glomerular thrombosis. Circulating white blood cell counts decreased within hours after induction of TGN in both WT and Mac-$1^{-/-}$ mice, but the recovery at day 4 was greater in Mac-$1^{-/-}$ mice than in WT counterparts, possibly as a compensation for reduced efficiency of renal neutrophil accumulation (Figure I in the online-only Data Supplement).

Together, the data indicate that Mac-$1^{-/-}$ mice exhibit reduced neutrophil accumulation and reduced susceptibility to TMA-associated endothelial injury, glomerular pathology,

Circulation
JOURNAL OF THE AMERICAN HEART ASSOCIATION

American Heart Association
Learn and Live

Mac-1 (CD11b/CD18) Links Inflammation and Thrombosis After Glomerular Injury

Junichi Hirahashi, Keiichi Hishikawa, Shinya Kaname, Naotake Tsuboi, Yunmei Wang, Daniel I. Simon, George Stavrakis, Tatsuo Shimosawa, Ling Xiao, Yutaka Nagahama, Kazuo Suzuki, Toshiro Fujita and Tanya N. Mayadas

Circulation 2009;120;1255-1265; originally published online Sep 14, 2009;
DOI: 10.1161/CIRCULATIONAHA.109.873695
Circulation is published by the American Heart Association. 7272 Greenville Avenue, Dallas, TX 72514
 Print ISSN: 0009-7322. Online ISSN: 1524-4539

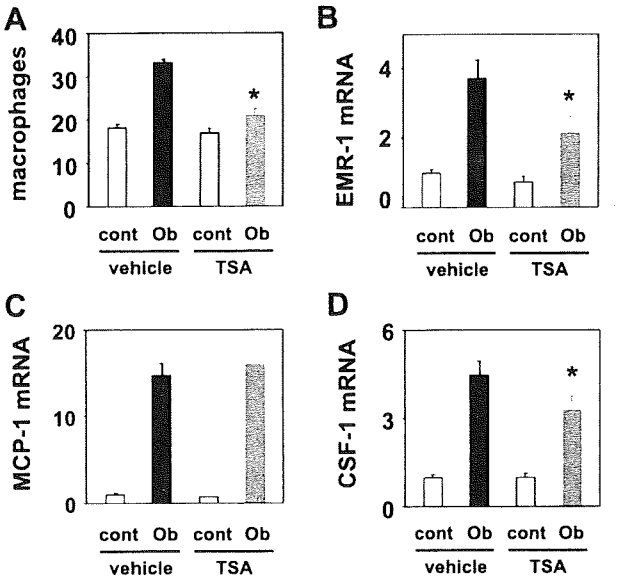

Fig. 6. Reduction in infiltration of macrophages and colony-stimulating factor (CSF)-1 mRNA levels in UUO mice by HDAC inhibition. *A*: mean number of F4/80-positive cells in the interstitium of the kidneys obtained 2 days after ureteral obstruction is indicated as means ± SE (n = 5). *P < 0.05 vs. values of obstructed kidneys obtained from mice treated with vehicle. The mRNA levels of epidermal growth factor-like molecule containing mucin-like hormone receptor 1 (EMR-1; *B*), monocyte chemoattractant protein (MCP)-1 (*C*), and CSF-1 (*D*) in kidneys obtained 2 days after ureteral obstruction from mice treated with vehicle or TSA were determined by RT-PCR. Values are means ± SE and were normalized to those for 18S and expressed as relative values of contralateral kidneys obtained from mice treated with vehicle; n = 5. *P < 0.05 vs. values of obstructed kidneys obtained from mice treated with vehicle.

of signals in various physiological and pathophysiological conditions. For example, changes in HDAC2 expression and activities have been shown to mediate neuronal development and memory formation (11, 28). In cardiac muscle, a transient increase in HDAC2 activities contributes to muscle hypertrophy after aortic banding (17). In addition, induction of HDAC4 modulates phenotype changes of skeletal muscle after denervation (34). However, little was known about regulation and function of HDAC in kidney diseases. In the present study, we demonstrate that HDAC1 and HDAC2 are transiently induced in renal tubular cells in the early phase of tubulointerstitial injury caused by UUO. The induction of HDAC1 and HDAC2 likely contributes to the reduced level of histone acetylation and altered gene expression in the tubular cells of the injured kidney. The present study suggests that CSF-1, a chemokine involved in the initiation of tubulointerstitial injury (8, 16, 20), may be regulated by the induction of HDAC1 and HDAC2 in injured tubules. This notion is supported by the observations that a HDAC inhibitor, TSA, attenuated the induction of CSF-1 in vivo and in vitro and that the knockdown of HDAC1 or HDAC2 in tubular cells significantly reduced CSF-1 induction by TNF-α. In addition, valproate, another HDAC inhibitor with a different chemical structure, also reduced CSF-1 induction by TNF-α. These findings suggest that HDAC1 and HDAC2, induced in the renal tubular cells, may modulate proinflammatory responses in the early stage of tubulointerstitial injury.

Indeed, inhibition of HDAC by TSA reduced macrophage infiltration and profibrotic changes after UUO. The inhibition of CSF-1 induction is likely to contribute to a reduction of macrophage infiltration by TSA, since knockdown of CSF-1 has been shown to reduce macrophage infiltration into the interstitium and the subsequent tubular injury (16, 20). In addition to the direct effects of HDAC inhibitor on renal tubular cells, immune-modulating effects of TSA may also play some role in decreased macrophage infiltration since HDAC inhibition has recently been demonstrated to regulate inflammation by modulating immune cells, including dendritic cells (30) and regulatory T cells (35).

A reduction in macrophage infiltration is likely to contribute to the antifibrotic effects of HDAC inhibition in the early stage of UUO. Although a subset of tissue macrophages in the late

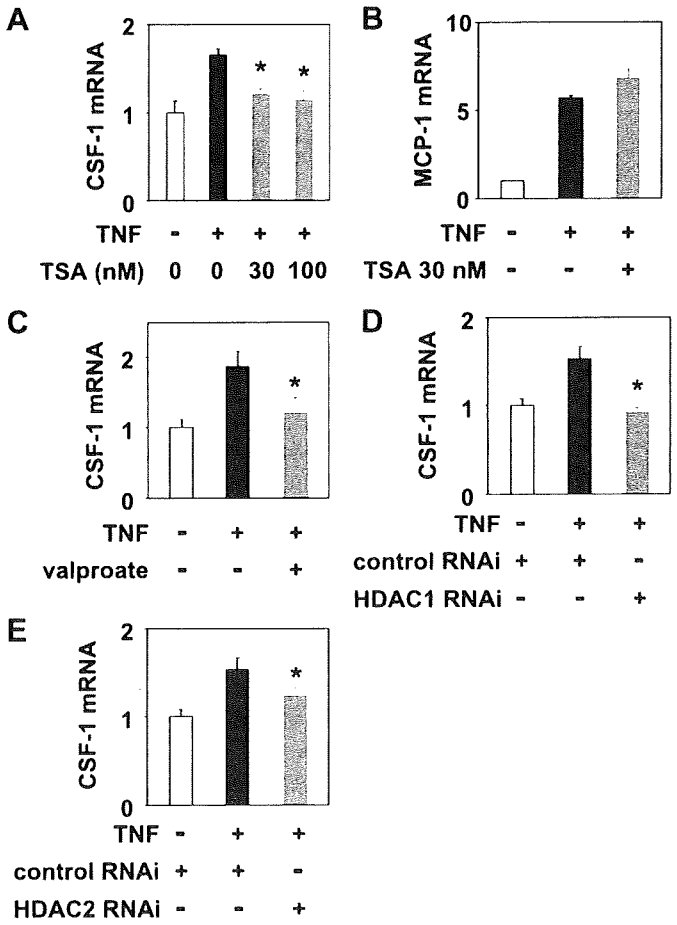

Fig. 7. Knockdown of HDAC1 or HDAC2 attenuates CSF-1 induction in renal tubular cells. *A*: NRK 52E cells were incubated with or without TSA (30 or 100 nM) in the presence of 10 ng/ml TNF-α for 24 h. The level of CSF-1 mRNA was determined by RT-PCR. Values are means ± SE and were normalized to those for 18S and expressed as relative values of control; n = 3–7. *P < 0.05 vs. values with TNF-α alone. *B*: NRK 52E cells were incubated with or without 30 nM TSA in the presence of 30 ng/ml TNF-α for 24 h. The level of MCP-1 mRNA was determined by RT-PCR. Values are means ± SE and were normalized to those for 18S and expressed as relative values of control; n = 8. *P < 0.05 vs. values with TNF-α alone. *C*: NRK 52E cells were incubated with or without sodium valproate (1 mM) in the presence of 30 ng/ml TNF-α for 24 h. The level of CSF-1 mRNA was determined by RT-PCR. Values are means ± SE; n = 7–8. *P < 0.05 vs. values with TNF-α alone. Renal tubular cells were treated with control or HDAC isozyme (HDAC1 in *D* and HDAC2 in *E*) Stealth RNAi (RNA interference) for 24 h. After further incubation with 30 ng/ml TNF-α for 24 h, the mRNA levels of CSF-1 were determined by RT-PCR. Values are means ± SE; n = 8. *P < 0.05 vs. values with TNF-α and control RNAi.

likely activate neutrophils.[5–7] However, the pathogenic role of neutrophils and molecular mechanisms underlying their potential contribution to the observed procoagulant state in TMA and other thrombotic disorders remains largely unknown.

Clinical Perspective on p 1265

In the present study, we developed a mouse model of thrombotic glomerulonephritis (TGN) induced by the sequential injections of anti-glomerular basement membrane (GBM) antibody and lipopolysaccharide that was characterized by renal endothelial cell damage, occlusive microvascular thrombosis, renal failure, and hematuria. These parameters are prominent in patients with HUS/thrombotic thrombocytopenic purpura.[3,8] The use of genetically modified mice, cell immunodepletion approaches, and functional blocking antibodies in this model allowed us to examine the molecular basis of inflammation-induced thrombosis in vivo and explore the pathogenesis of this clinically important disease. We demonstrate that neutrophils play a primary role in disease pathogenesis. We provide evidence that Mac-1, a member of the leukocyte-specific CD18 integrin family, promotes neutrophil recruitment, endothelial injury, glomerular thrombosis, and acute renal failure by regulating the release and/or activity of the serine proteinase neutrophil elastase (NE). We show that platelets initially preserve the integrity of the glomerular microvasculature after Mac-1–mediated neutrophil recruitment and injury, whereas subsequent neutrophil engagement of platelet glycoprotein (GP)Ibα via Mac-1 potently induces thrombosis.

Methods

Mice

Gene-deleted mice backcrossed to C57Bl/6 are denoted as B6 with an F number designating the number of generations the animals were backcrossed to C57Bl/6. Mac-1–deficient (Mac-1$^{-/-}$) mice[9] are B6F9 and were bred and maintained in the Viral Antigen Free facility at the Longwood Medical Research Center animal housing facility at Harvard Medical School. NE-deficient mice (B6F10)[10] were bred in the Viral Antigen Free facility at the Harvard School of Public Health animal housing facility and maintained in the Longwood Medical Research Center facility. Age-matched wild-type (WT) C57Bl/6 mice (Jackson Laboratory, Bar Harbor, Me) were used for all of the aforementioned C57Bl/6 gene–deleted animals. Experimental procedures were approved by the Animal Care and Use Committee of Harvard Medical School, Boston, Mass.

Generation of TGN

Rabbit antibody against mice GBM (anti-GBM serum) was prepared by immunizing rabbits with mouse GBM (Covance Research Products Inc). Control rabbit serum was purchased from Sigma, St Louis, Mo. Anti-GBM serum was incubated at 56°C for 30 minutes to inactivate complement and was filter sterilized. Male C57Bl/6 mice were injected twice via tail vein with 300 μL anti-GBM serum or normal rabbit serum at 1-hour intervals. Fifty micrograms of lipopolysaccharide from phenolic extracts of *Salmonella typhimurium* (CalBiochem, La Jolla, Calif) in sterile PBS was injected into mice via the tail vein 2 hours after the second anti-GBM serum injection. Peripheral blood was collected from the retroorbital plexus of anesthetized mice in glass tubes to obtain serum and in EDTA-containing vials to collect whole blood. The animals were euthanized by CO_2 inhalation, and both kidneys were harvested for histological analysis at the indicated times after lipopolysaccharide injection. All experimental procedures were performed in 6- to 8-week-old male mice because animals >10 weeks of age were more resistant to disease induction.

Immunodepletion of Neutrophils and Platelets and Anti-M2 Antibody Treatment

For immunodepletion of neutrophils, a rat anti-mouse monoclonal antibody against the neutrophil maturation antigen Gr-1 (BD Biosciences/Pharmingen) was used. WT mice were injected intraperitoneally twice with 100 μg of anti-Gr-1 antibody in 200 μL PBS at 24 hours before and after disease induction. A rat IgG2b (R&D Systems, Minneapolis, Minn) was used as an isotype control. The platelet-depleting anti-GPIbα antibody and isotype rat IgG control were purchased from Emphret (Wurzburg, Germany). WT or Mac-1 knockout mice were injected intravenously with 40 μg anti-GPIbα or rat IgG in PBS 12 hours before disease induction. WT mice were injected intravenously with 100 μg of affinity-purified, peptide-specific polyclonal antibody (termed anti-M2) to the Mac-1 binding site for GPIbα[11] or nonimmune rabbit IgG antibody 1 hour before the first injection of anti-GBM.

Peripheral Blood Cell Count and Differentials

Blood collected in EDTA was used in MBC biochemistry (Tokyo, Japan) to generate a complete blood count with cellular differential.

Functional Assessment of Renal Injury

Serum values for creatinine, blood urea nitrogen (BUN), and lactate dehydrogenase (LDH) were obtained with a Hitachi 7700 Automatic Analyzer at MBC (Tokyo, Japan). Hematuria grading was conducted by dipstick analysis with the use of Uro-paper (Eiken Chemical Co, Tokyo, Japan). For collection of serum, blood sampled from the retroorbital plexus of mice was collected in glass tubes, kept at 4°C for 30 minutes, and centrifuged.

Histological and Immunohistochemical Analysis of Renal Tissue

Coronal sections (4 μm) of paraffin-embedded kidneys were stained with periodic acid–Schiff (PAS) or Masson trichrome reagent for analysis of glomerular and interstitial injury. Prevalence of glomerular capillary thrombosis (%) equaled total number of glomeruli with thrombus in at least 1 glomerular capillary per total number of glomeruli.[12] Fibrin deposition was detected by phosphotungstic acid–hematoxylin (PTAH) staining of paraffin renal sections.

Paraffin-embedded kidney sections were stained with rat monoclonal antibody to CD34 (GeneTex, Inc, San Antonio, Tex). The staining intensity within the capillary walls in glomeruli or the interstitium was scored on a scale of 0 to 3 (0, none; 1, weak; 2, moderate; 3, strong) by an observer blinded to the identity of the sample. Platelets were stained with goat polyclonal antibody to integrin αIIb (Santa Cruz Biotechnology Inc, Santa Cruz, Calif).

Chloroacetate Esterase Reaction for Neutrophil Enumeration

Paraffin sections from kidneys were deparaffinized and incubated in freshly prepared chloroacetate solution containing 0.0125% Naphtol AS-D (Sigma) and 0.0625% Fast Blue BB salt (Sigma) in phosphate buffer (pH 7.3) for 1.5 hours in the dark. The number of esterase-positive neutrophils in at least 50 glomeruli per section was calculated and reported as the total number of neutrophils per glomerulus cross section.

Multiple Cytokine and Chemokine Analysis

Homogenates from mice kidney at indicated times were subjected to the Bio-Plex suspension array system (Bio-Rad Laboratories, Hercules, Calif) to measure the concentration of 32 cytokines: granulocyte monocyte colony-stimulating factor, granulocyte colony-stimulating factor, interleukin (IL)-1α, IL-1β, IL-2, IL-3, IL-4, IL-5, IL-6, IL-9, IL-10, IL-12p40, IL-12p70, IL-13, IL-15 IL-17, IL-18, interferon-γ, tumor necrosis factor-α, monocyte chemotactic protein-1, RANTES (regulated upon activation, normal T cell

Table 1. Intrarenal Cytokine Profile in WT and Mac-1–Deficient Mice at 4 Hours After Induction of TGN

	WT Control	WT TGN	Mac-1$^{-/-}$ Control	Mac-1$^{-/-}$ TGN
IL-1α	22.2±6.0	47.3±4.7*	17.4±1.6	48.0±2.6†
IL-1β	151.4±15.8	208.5±13.9*	102.8±9.7	229.1±13.1†
IL-6	22.6±4.7	181.2±46.9*	15.6±1.2	253.7±35.3†
IL-12 (p40)	7.3±1.0	124.9±26.8*	6.1±0.8	95.3±15.3†
G-CSF	1.1±0.3	310.1±43.8*	0.6±0.1	369.1±58.4†
KC	4.0±1.1	1282.1±293.5*	3.1±0.2	1682.4±491.2†
RANTES	64.6±10.9	550.9±85.7*	52.5±4.9	546.5±26.5†
MCP-1	42.0±6.7	411.7±85.7*	35.1±2.9	488.5±120.9†
MIP-1β	26.3±5.1	56.4±5.4*	18.1±2.3	56.2±3.2†
IL-15	181.2±13.8	340.4±53.8*	88.9±25.0	290.5±51.1†
FGF basic	326.2±43.9	2329.5±794.5*	730.1±288.8	2131.5±458.4†
LIF	7.6±0.8	58.5±7.2*	3.85±0.58	64.9±10.0†
M-CSF	19.7±1.3	88.1±6.5*	20.8±0.3	95.2±12.6†
MIG	2628.4±209.6	63 889.8±13 826.4*	2777.3±901.6	62 931.0±4478.1†
MIP-2	6.4±0.6	265.1±41.1*	4.2±0.7	342.7±77.3†
PDGF-BB	1300.8±149.9	7742.9±1491.0*	3808.4±728.0	8805.2±1370.8†

Data are mean±SEM; n=4 per group. G-CSF indicates granulocyte colony-stimulating factor; RANTES, regulated upon activation, normal T cell expressed and secreted; MCP-1, monocyte chemotactic protein-1; MIP-1β, macrophage inflammatory protein-1β; FGF, fibroblast growth factor; LIF, leukemia inhibitory factor; M-CSF, macrophage colony-stimulating factor; MIP-2, macrophage inflammatory protein-2; and PDGF, platelet-derived growth factor. TGN was induced in WT or Mac-1$^{-/-}$ mice, and kidneys were harvested 4 hours later. Cytokine concentrations in pg/mg of total protein in kidney homogenates were measured by the Bio-Plex System.

*P<0.05 compared with WT control.

†P<0.05 compared with Mac-1$^{-/-}$ control.

NE release and/or activity and stimulates the accumulation of platelets that initially function to preserve vessel integrity in the context of neutrophil-mediated vascular damage. However, subsequent interaction of neutrophil Mac-1 with GPIbα on deposited platelets promotes thrombosis, a major aspect of renal injury in this model (Figure 5).

We developed a model of TMA in mice that has functional outcomes and laboratory features that resembled HUS in humans so that the molecular cross talk between inflammation and thrombosis, 2 prominent features of HUS, and the pathogenesis of this disease can be explored. Many aspects of HUS were recapitulated in our model, such as endothelial injury, glomerular thrombosis, thrombocytopenia, neutrophilia, renal failure, and LDH elevation. However, anemia, a major characteristic of HUS, was not significant in this mouse model, as was also the case in published rat models.[21,22] This may be because the glomerular intravascular hemolysis is not severe enough to manifest as systemic anemia because glomerular thrombosis is localized and less extensive in the rodent models compared with the human disease. Glomerular endothelial cell damage is a predominant feature of TMA in humans. CD34 served as a sensitive readout of glomerular endothelial injury that also correlated with the extent of leukocyte infiltration and thrombosis. The reduction of CD34 in TGN correlated with an increase in renal levels of E-selectin, a selective marker of endothelial activation. Anti-GBM antibody or lipopolysaccharide alone was not sufficient

Table 2. NE-Deficient Mice Are Protected From TGN

	WT	NE$^{-/-}$
PAS, %	83.55±4.88	60.78±5.65*
Hematuria grade	2.86±0.14	1.43±0.30*
Creatinine, mg/dL	0.30±0.05	0.17±0.02*
BUN, mg/dL	153.70±28.70	78.90±9.80*
LDH×10^3, IU/L	2.00±0.26	1.11±0.12*
PMNs/glomerulus cross-section	5.74±1.04	0.91±0.15*

Data are mean±SEM. TGN was induced in NE-deficient mice. Quantification of glomerular PAS, hematuria, functional markers (BUN, serum creatinine, LDH), and glomerular polymorphonuclear neutrophil (PMN) accumulation in WT and NE$^{-/-}$ mice are given. All analyses were done at 96 hours after TGN except glomerular neutrophil recruitment, which was evaluated at 4 hours after TGN induction.

*P<0.05 compared with WT.

Table 3. Quantification of Elastase-Digested Fibrin Degradation Products in Plasma Samples

Day	0	1	2	4
WT, μg/mL (n)	0.06±0.06 (4)	2.26±0.17 (12)	1.69±0.19 (5)	1.97±0.28 (4)
Mac-1$^{-/-}$, μg/mL (n)	0.01±0.01 (4)	1.68±0.16 (12)	1.04±0.29 (4)	2.30±0.67 (4)
P	0.40	0.02	0.09	0.66

Data are mean±SEM. TGN was induced in WT or Mac-1$^{-/-}$ mice, and plasma from mice at the indicated times after TGN was examined for NE activity by examining fibrin degradation products reported to be specifically generated by granulocyte-elastase (e-XDP). (n) represents the number of animals evaluated.